Remote sensing the plasmapause by means of monitoring conjugated ionospheric phenomena

(Magnetosphere-ionosphere coupling processes in the sub-auroral topside ionosphere)

Balázs Heilig

Institute of Earth Physics and Space Science, Sopron, Hungary

Eötvös Loránd University Space Research Group, Budapest, Hungary

Magnetosphere-Ionosphere coupling

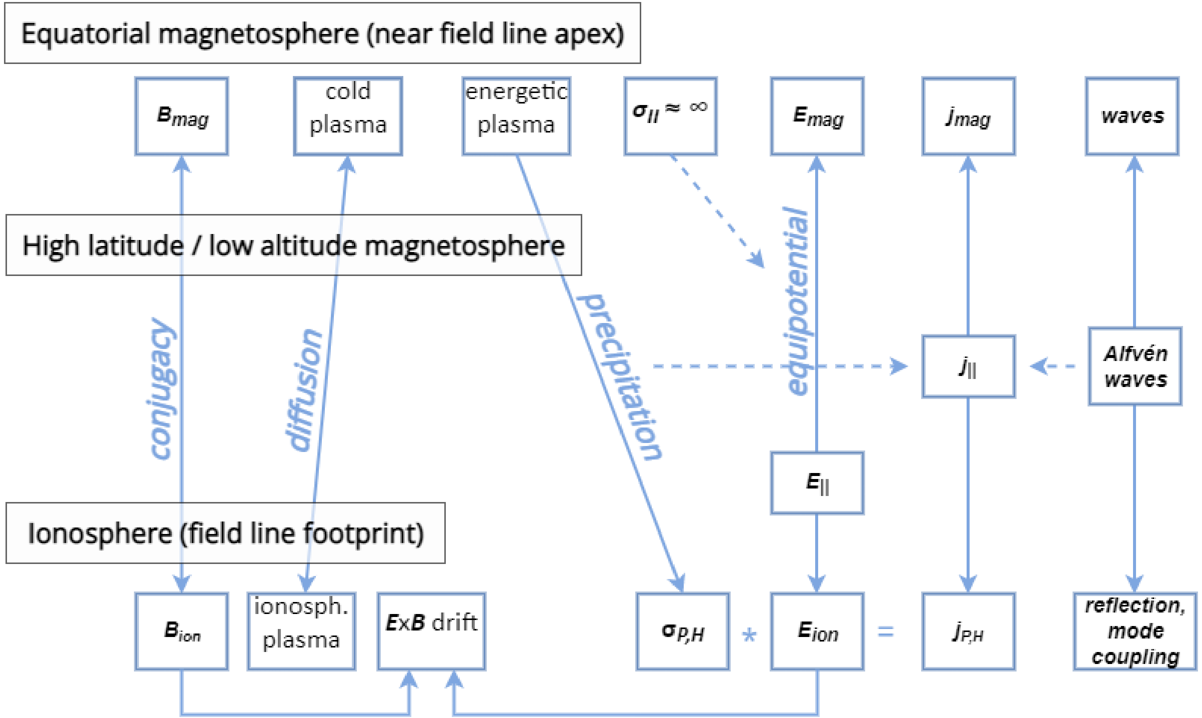

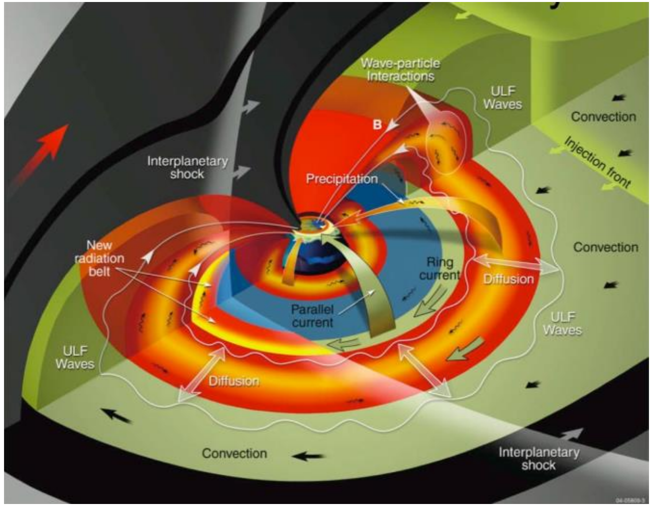

Credit: NASA

Outline

- Discovery of ionospheric phenomena and their relations to the plasmapause (a historical introduction)
- Phenomology of PP related ionospheric phenomena, their possible generation mechanisms in the light of M-I coupling
- The use of LEO (Swarm) observations in monitoring plasmapause dynamics

Outline

- **Discovery of ionospheric phenomena and their relations to the plasmapause (a historical introduction)**
- Phenomology of PP related ionospheric phenomena, their possible generation mechanisms in the light of M-I coupling
- The use of LEO (Swarm) observations in monitoring plasmapause dynamics

Discovery of the plasmapause (1963)

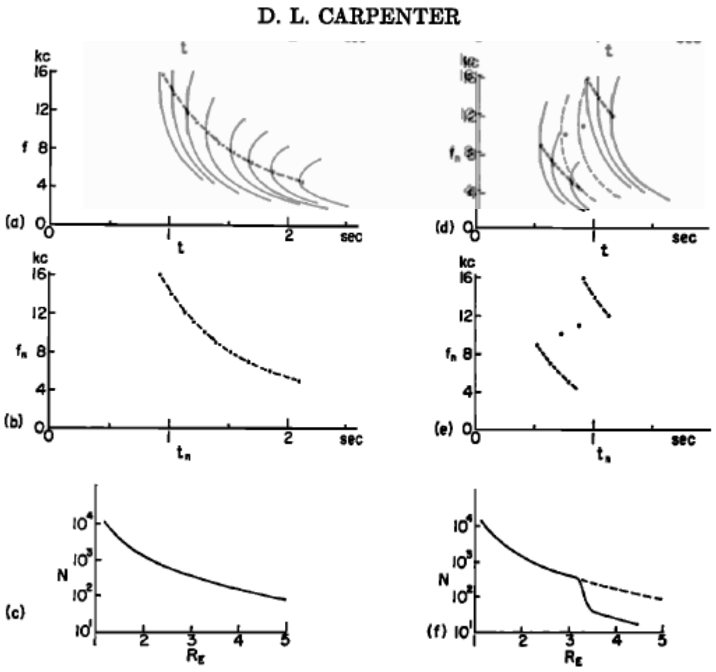

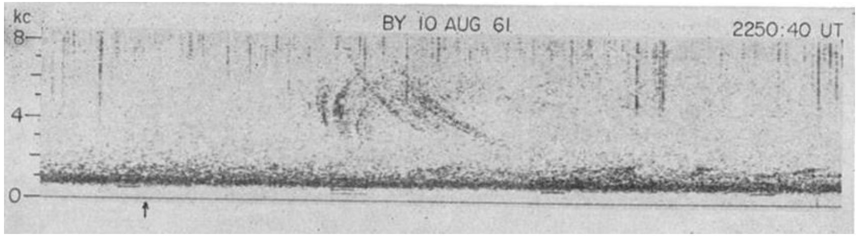

Knee whistler recorded at Byrd, Antarctica

‚Ordinary' and ‚knee' whistlers

… and the inferred density profile (Ne vs. L)

(Carpenter, 1963)

Early observations of the plasmapause related ionospheric phenomena (#1 MIT)

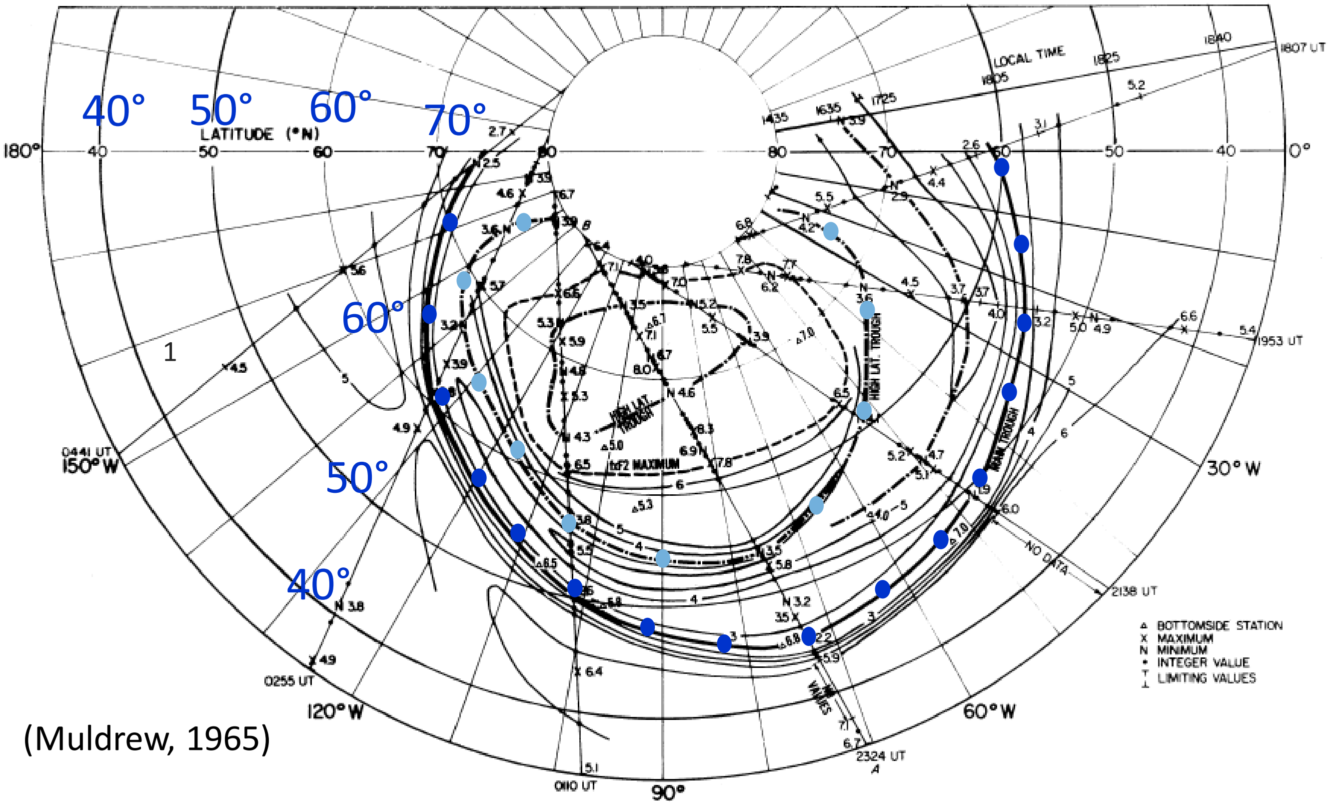

(Muldrew, 1965)

f_xF2: critical frequency of extraordinary mode wave propagation

$f_xF2 \sim \mathrm{sqrt}(Ne)$

Main Ionospheric Trough (MIT) (Alouette 1, 1962.10.24-25, LT ~ 18:00)

High-latitude trough

Early observations of the plasmapause related ionospheric phenomena (#1 MIT)

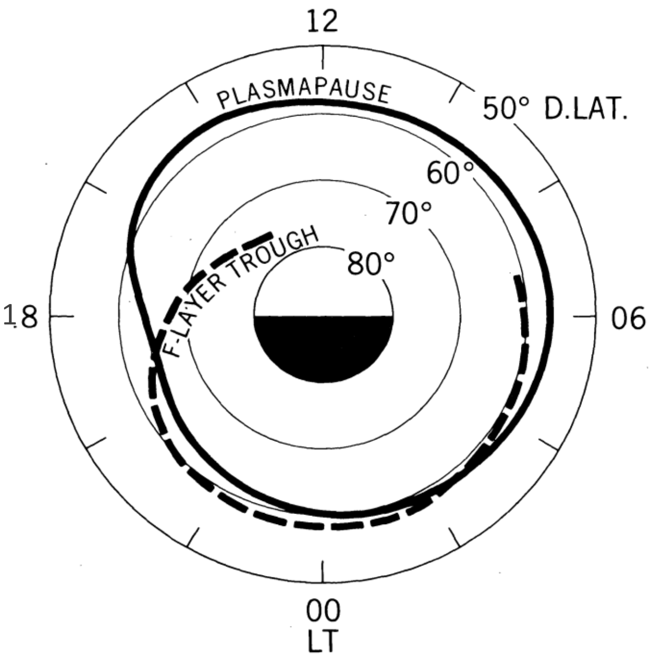

(Taylor and Walsh, 1972)

Both sensitive to Kp variation

$L = 4 \quad \sim \quad \Lambda = 60°$ (nightside)

A comparison of the diurnal variation observed in the main ionospheric (F2-layer) trough (dashed curve) and the average position of the plasmapause deduced from ground-based VLF recordings (solid curve).

– – – **MIT**: Alouette I, November 1962 to March 1963, with Kp = 2 (after Jelly and Petrie, 1969). (Similar trough found in total ion density, Sharp, 1966, ion trap)

—— **PP**: ground VLF whistlers, July and August 1963, with Kp = 2-4 (after Carpenter, 1966).

Early observations of the plasmapause related ionospheric phenomena (#2 SETE) (Brace and Theis 1973)

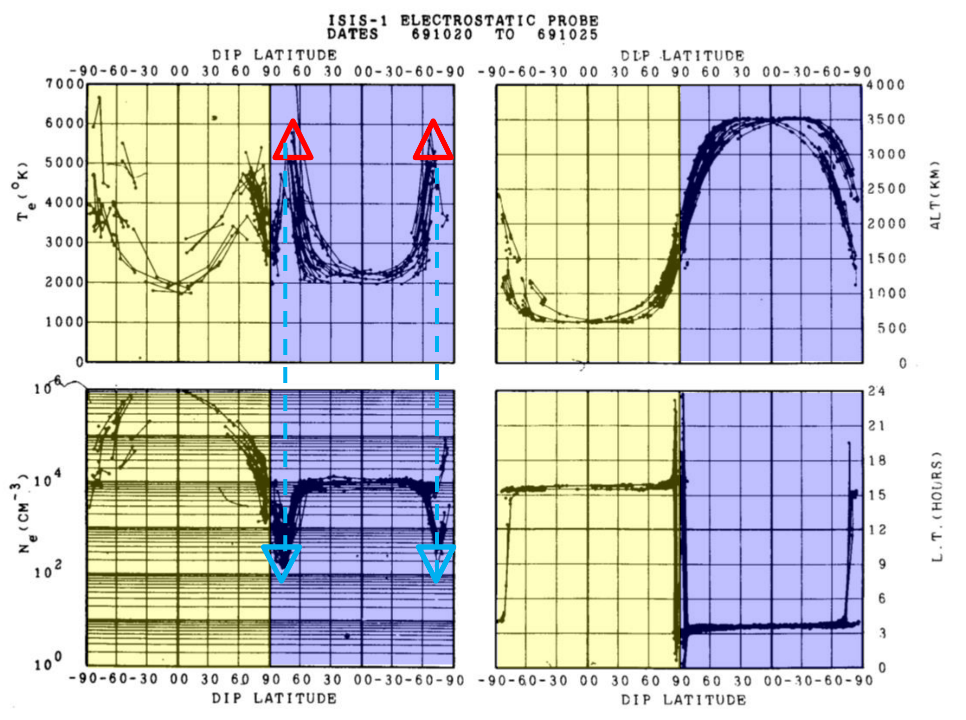

Latitudinal profiles of Te and Ne
(ISIS-1, 1969.10.20-1969.10.25)

Nightside (LT ~ 04) density deplitions
Co-located Te peaks
Sub-Auroral Temperature Enhancement (SETE term by Prölls**)**
Normally **within the PP gradient**

altitude: 1,500 - 3,000 km

Observed vertical temperature gradient:
1K/km → heat conducted downward

Early observations of the plasmapause related ionospheric phenomena (#3 LIT) (#4 WhB)

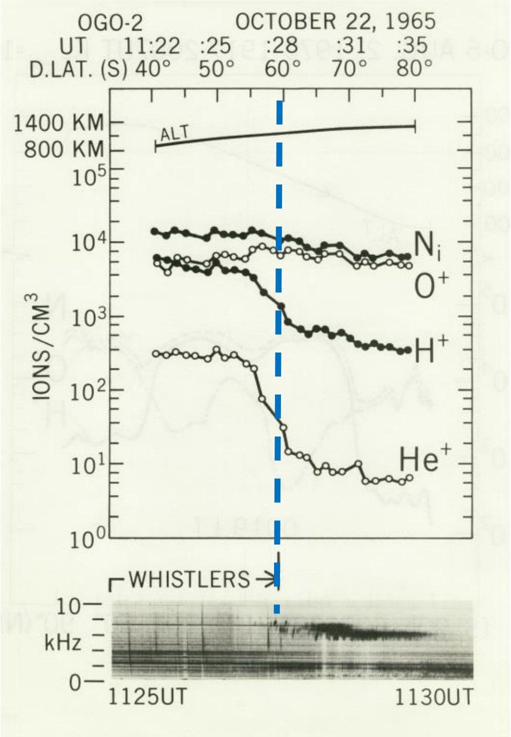

(Taylor and Walsh, 1972)

Ion composition and VLF whistler results both observed by OGO-2, for a PP crossing near 60° dipole latitude.

Note that the **last observable whistler** occurs near 1128 UT, as the concentrations of H+ and He+ (light ions) are falling to background levels: **Light Ion Trough** (**LIT**)

Note also that O+ as well as the total ion density, Ni (= Ne) reflect no evidence of the light ion trough-plasmapause.

Early observations of the plasmapause related ionospheric phenomena (#3 LIT)

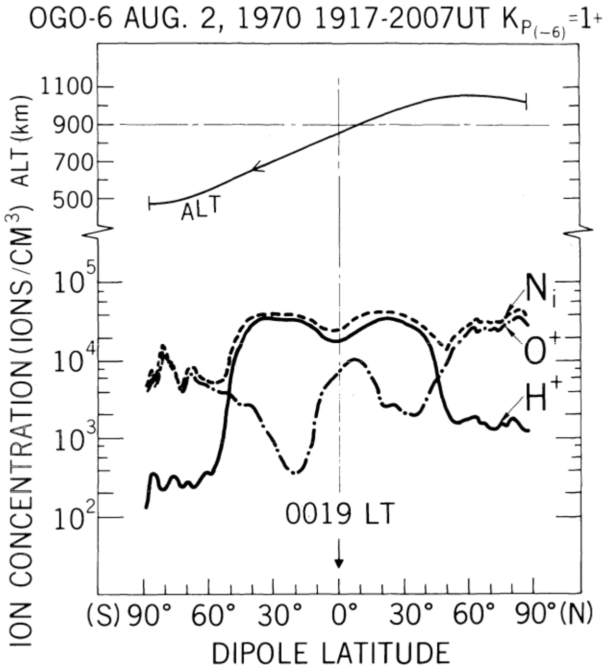

(Taylor and Walsh, 1972)

LIT example in H+ observed near midnight LT, with trough boundaries near 55-60° in both the N and S hemispheres.

Total ion density distribution, Ni
(mass range 1-45 amu, mainly O+ and H+).

Pronounced LIT at both altitudes.

A comparison of the diurnal variation in LIT (OGO-6) and the PP deduced from ground-based VLF recordings (dashed curve).

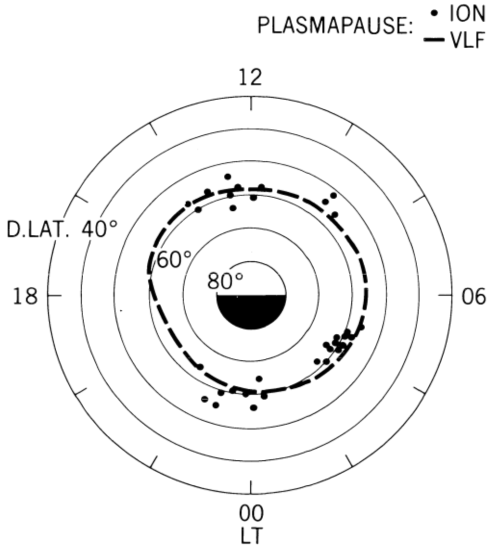

Early observations of the plasmapause related ionospheric phenomena (PP-LIT)

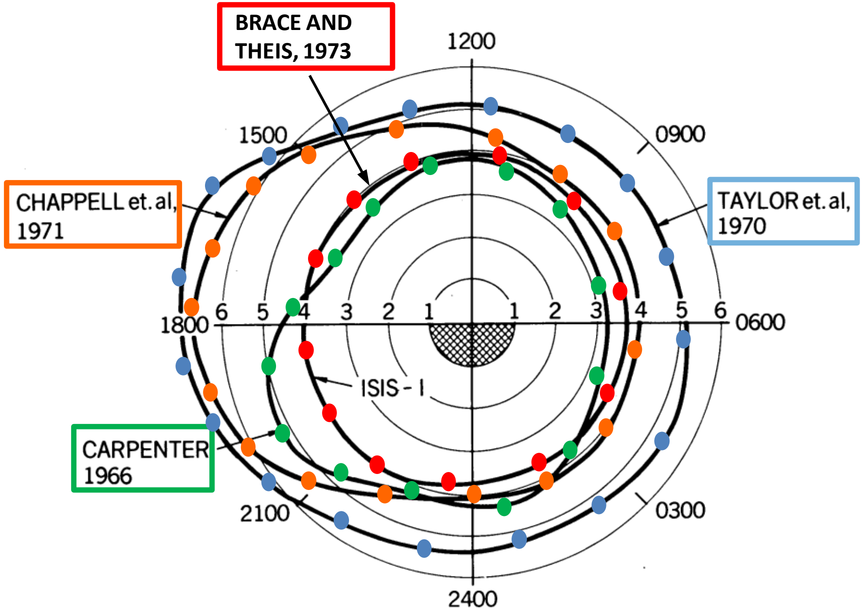

(after Brice and Theis, 1973)

(all different epochs!, different altitudes)

A comparison of the diurnal variation of PP and related boundaries

CARPENTER, 1966: VLF whistlers (ground-based), Kp = 2-4,1963

TAYLOR et al., 1970: LIT Kp ≤ 3, 1966-67 (H+, He+, OGO-3)

CHAPPELL et al, 1971: LIT, (ion mass spectrometer, OGO-5)

BRACE and THEIS, 1973: LIT (Langmuir probe, ISIS-1)
no bulge! right above the ionosphere

No clear correspondence, only on the nightside.
Afternoon: F2 MIT, ISIS LIT PP, VLF PP all different

Early observations of the plasmapause related ionospheric phenomena (#5 PJ/SAID)

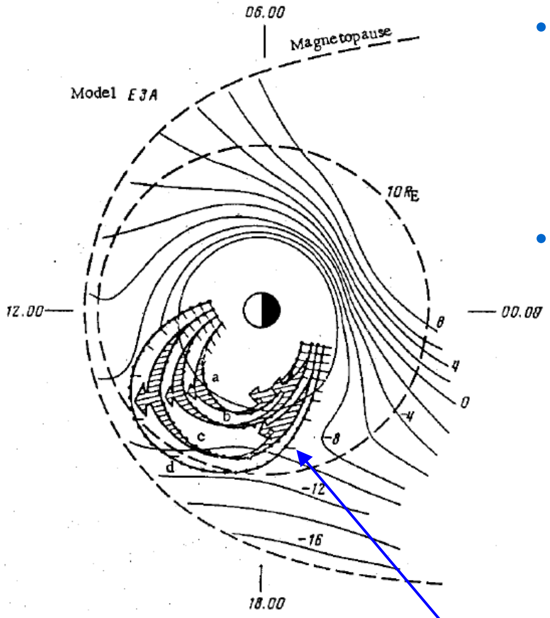

(Galperin et al., 1975)

Cosmos-184 trajectories

- strong horizontal drift equatorward of the auroral oval (polarization jets, PJ) (COSMOS-184).
  (Galkin et al., 1973)
- rapid subauroral ion-drift (SAID) (Atmosphere Explorer C)
  (Spiro et al., 1979)

→ related to stormtime PP dynamics
(Galperin et al., 1975)

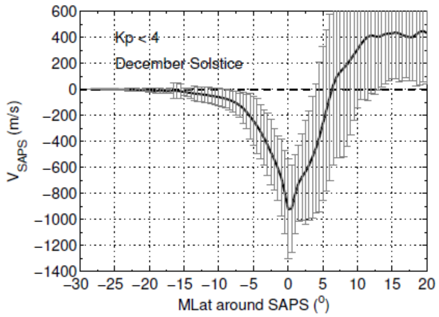

(Wang and Lühr, 2013)

Stable Aurora Red (#6 SAR) arcs

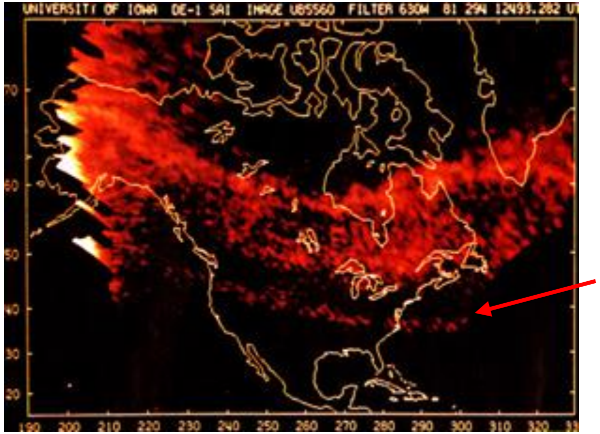

SAR arc

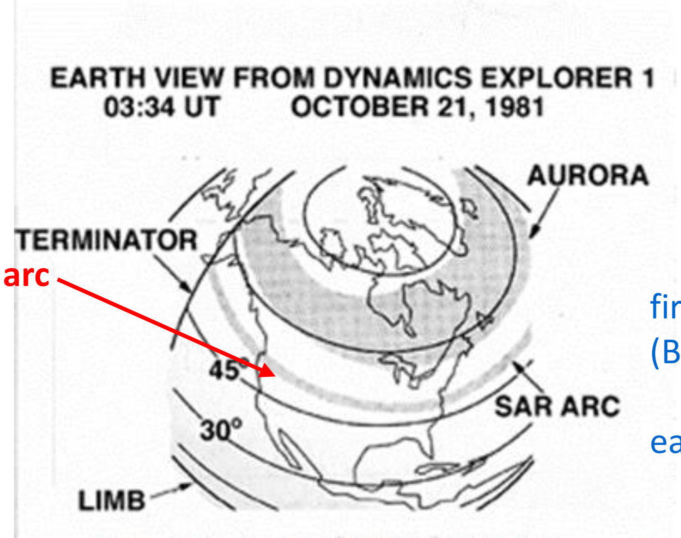

(Craven et al, 1982) DE 1 observation

first observation from ground: (Barbier, 1958)

early 1970s: related to the PP

Subauroral phenomenon
atomic O, excited ^{1}d level: emission at 630 nm.
needed: 2 eV ← Te > 23 000 K:
narrow in latitude, elongated in longitude
alt. range: 200-400 km

Heat is conducted downard from the magnetosphere

- observed (e.g. Brace and Theis, 1973)
- coincident with enhanced Te (**SETE**)

Distribution of small-scale field-aligned currents (#7 SSB)

CHAMP SSFAC boundary

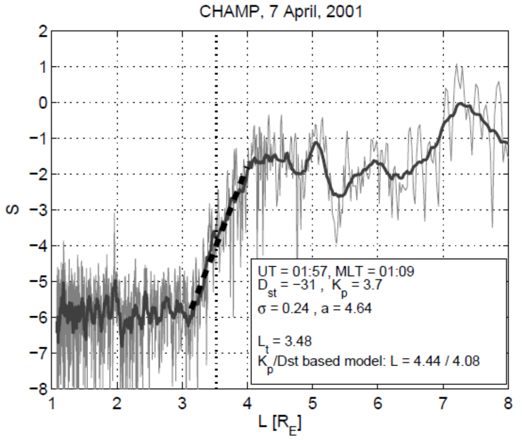

(Heilig and Lühr, 2012)

$$S = \left\langle \log_{10} j_{\parallel}^{2} \right\rangle_{20\,\mathrm{s}}$$

$j_{\parallel}$ is SSFAC (high-pass filtered, f_c = 0.25 Hz)

Intensity of small-scale field aligned currants changes orders of magnitude in the subauroal topside ionosphere (closely located to the PP, see later)

(Heilig and Lühr, 2012; 2018)

Swarm example with simultaneous MIT observation

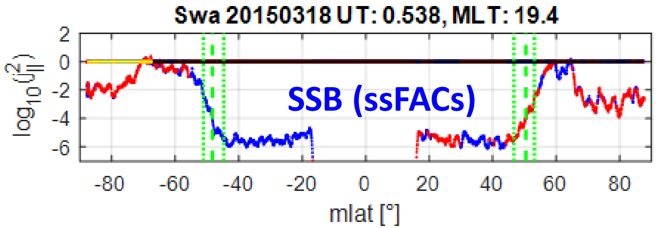

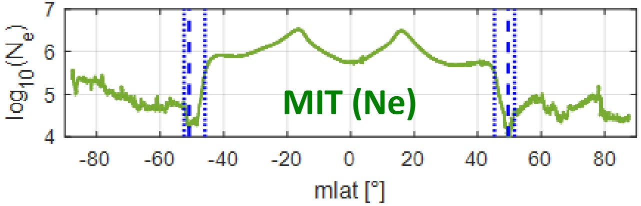

Plasmapause and related boundaries

PP (knee): Carpenter, 1963 (ground whistler)

#1 MIT (*Ne*): Main ionospheric trough: Muldrew, 1965 (Alouette I topside sounder)
#2 SETE (*Te*): At topside (1000 km): Miller, 1970 (Explorer 22 Langmuir probe) (heat conduction)
MIT (*Ni*): Ion trough (in total ion density): Sharp, 1966 (Alouette? ion trap)
#3 LIT (N_{H+He+}): Light ion trough: Taylor, 1972 (OGO observations)
#5 SAID/PJ (SAPS) (v_{west})**:** Sub-auroral ion drift (polarization streams)
#4 WhB: High-latitude limit of whistler occurrence
#6 SAR (stable auroral red) **arcs**: Barbier, 1958; **their relation to PP**: Carpenter, 1971; Cornwall et al., 1971
#7 SSB (equatorward boundary of small-scale field aligned currents (Heilig and Lühr, 2012)

Basu et al., 2005

#8 precipitation boundary ~ equatorward edge of the auroral oval (poleward of MIT),

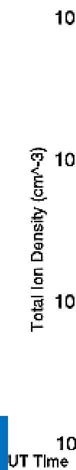

Outline

- Discovery of ionospheric phenomena and their relations to the plasmapause (a historical introduction)
- **Phenomology of PP related ionospheric phenomena, their possible generation mechanisms in the light of M-I coupling**
- The use of LEO (Swarm) observations in monitoring plasmapause dynamics

Plasma boundary layer (plasmapause)

Corotation

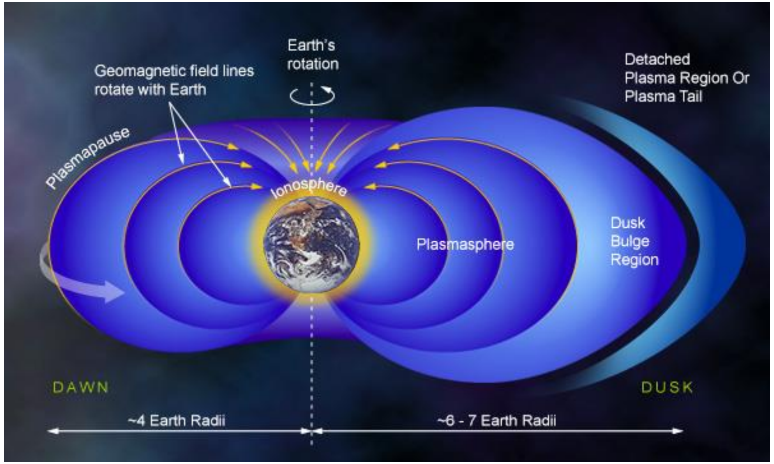

Credit: windows2universe.org

Global convection

Global convection + corotation

Equatorial cut looked from above the Noth pole

\+

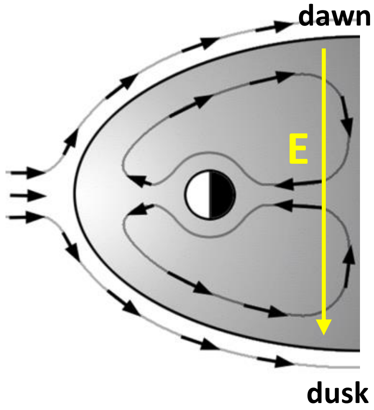

=

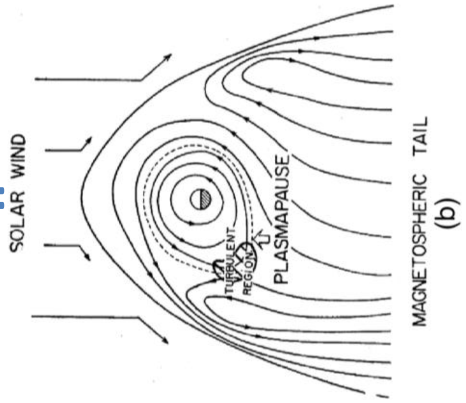

Two-cell global convection

Three-cell global convection (Nishida, 1966)

Plasmapause
- sharp density drop near L = 2..6 or beyond depending on geomagnetic activity

Plasmapause separates
- the plasma corotating with the Earth from
- the global convection dominated plasma

Magnetosphere – ionosphere mapping

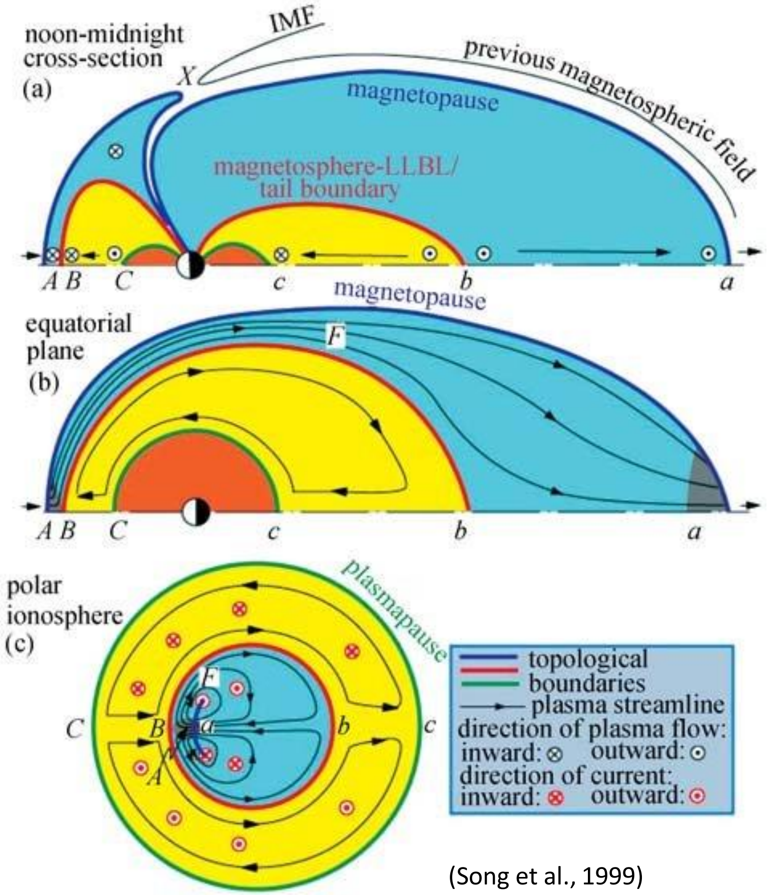

(Song et al., 1999)

Plasmasphere
Outer magnetosphere
LLBL / tail

outermost innermost

innermost outermost

plasmasphere is equatorward of the yellow ring

Sub-auroral ionosphere – plasma boundary layer

magnetosphere (inertial frame fixed to the Sun-Earth line)

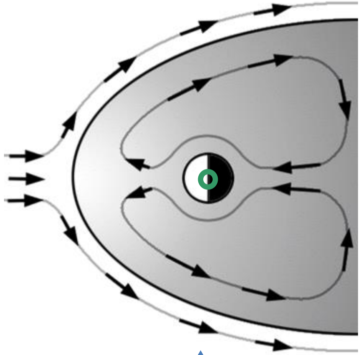

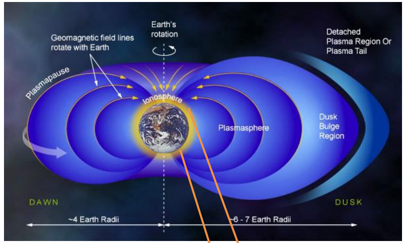

Magnetospheric plasma **collisionless**

→ field lines are **equipotential**

→ magnetospheric and ionospheric **E-fields** are coupled through field lines

→ **ExB drifts** are also coupled

Diffusion

- dayside refilling
- night side loss

ionosphere

(**frame corotating** with the Earth)

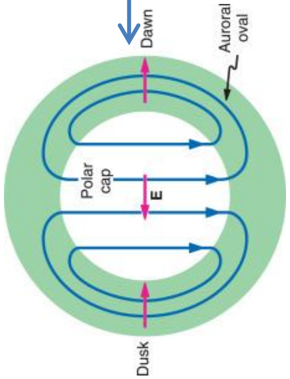

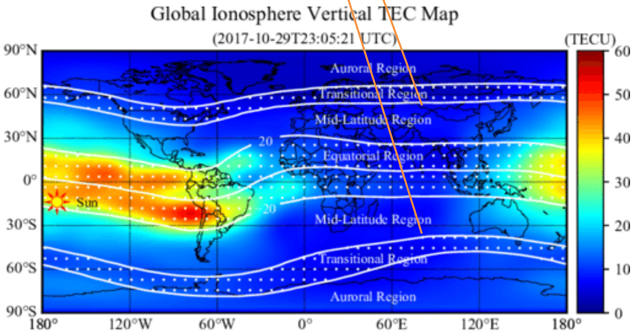

(Liang et al., 2019)

The plasmapause maps

- somewhere into the **sub-auroral ionosphere**
- in the transitional region (between **convection** dominated auroral region and mid-latitudes where **corotating** field lines map)
- this is where MIT is observed and formed

The Midlatitide (or Main) Ionospheric Trough (MIT) seasonal dependece

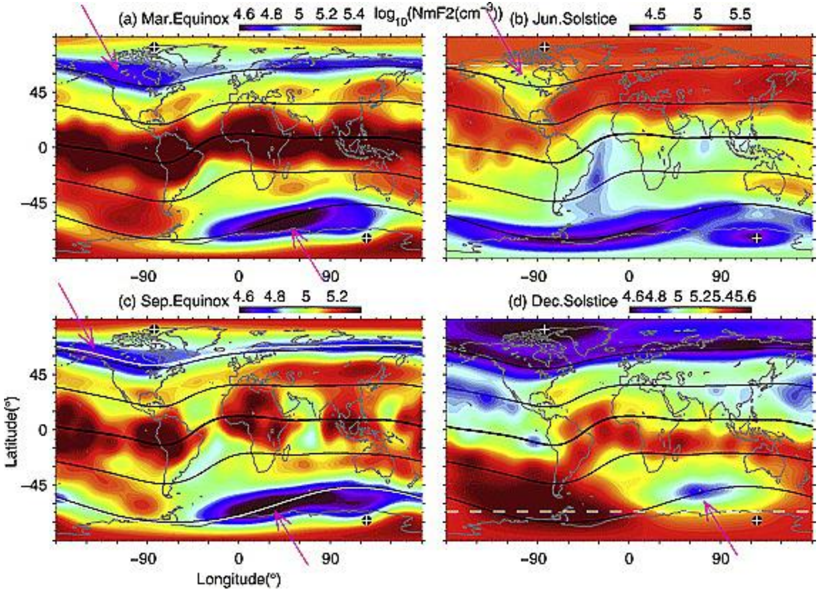

NmF2 maps for four seasons (He et al., 2011)

(COSMIC constellation of 6 sats, RO, 2006-2010, altitude: 500-800 km, Kp<3)

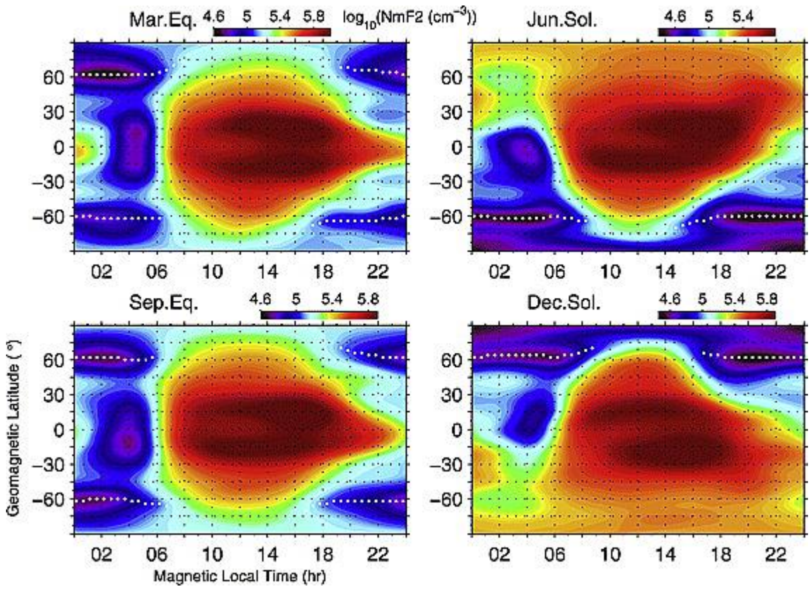

- winter and equinox months
- nighttime
- longitudinal variation (S hemisphere!)

Sub-auroral ionosphere – mid-latitude trough

magnetosphere

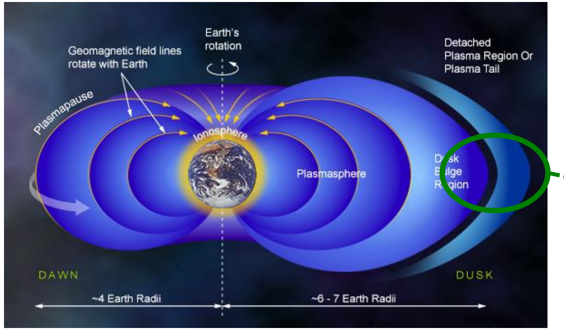

bulge

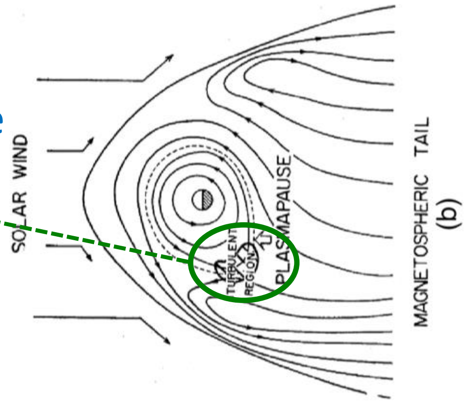

ionosphere

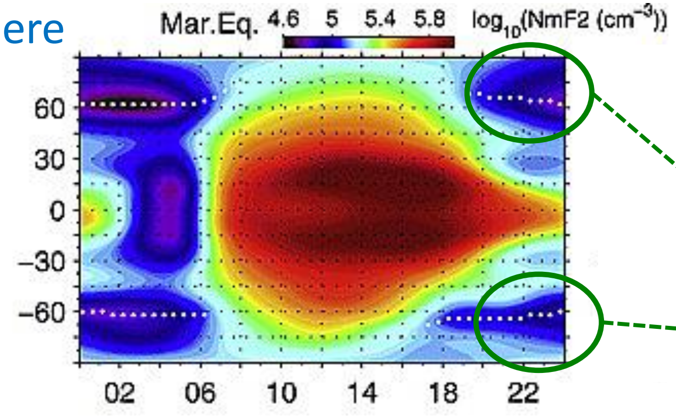

(He et al., 2011)

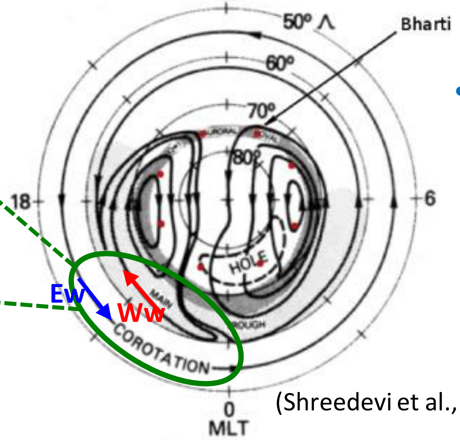

(Shreedevi et al., 2019)

Flow stagnation leads to

- magnetosphere: dusk side plasma **accumulation** > **bulge** formation (surplus plasma)
- **balance of the E-fields** > if in darkness > prolonged **recombination** (collisions!) > plasma **depletion** > **trough** (MIT) (plasma deficit)
- **SETE**? frictional heating + heat conducted downward + low density?

The Midlatitide (or Main) Ionospheric Trough (MIT) dependence on geomagnetic activity

MIT position modulated by Kp

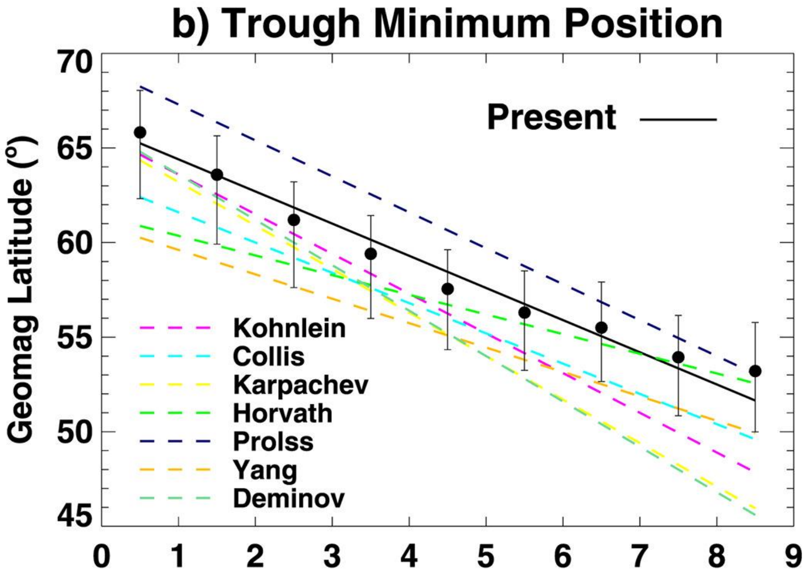

(Aa et al., 2020)

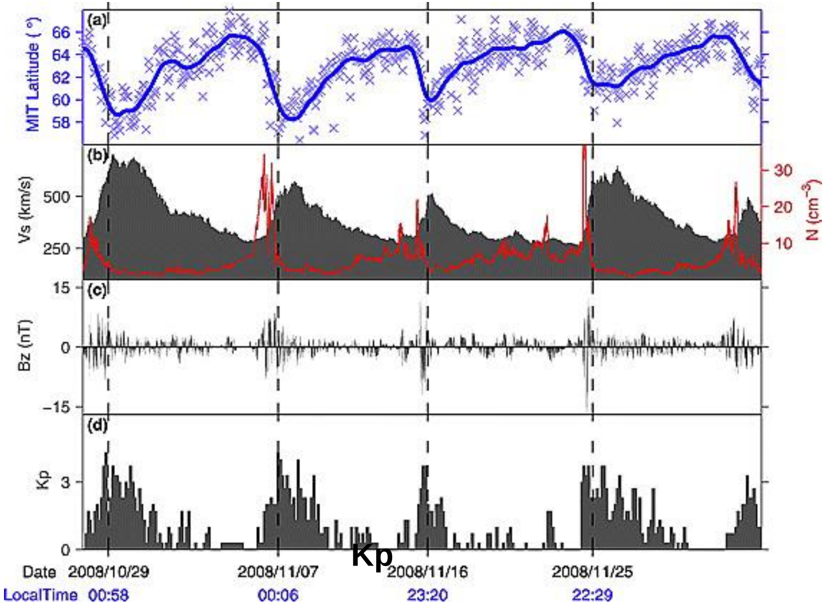

MIT location modeulated by Kp 2008.10.28-12.05, CHAMP, LP Ne, altitude: 330 km (He et al., 2011)

Kp increase ~ increase in global convection

Sub-auroral ionosphere – mid-latitude trough

magnetosphere

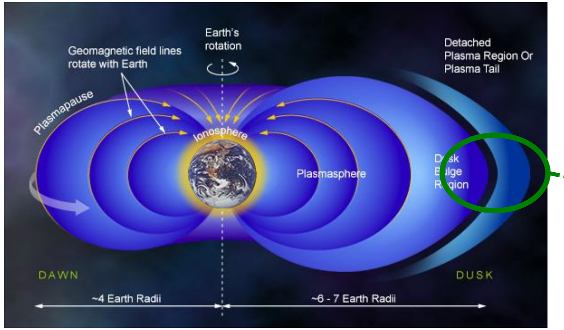

bulge

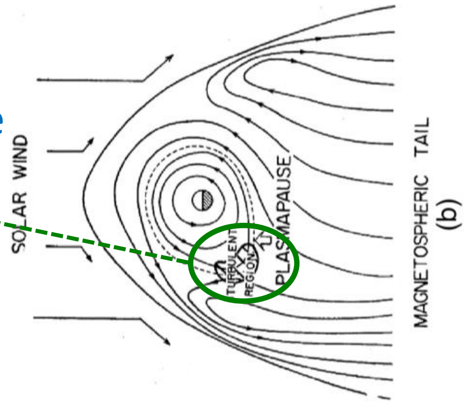

stronger convection E-field

- plasmasphere contracts

ionosphere

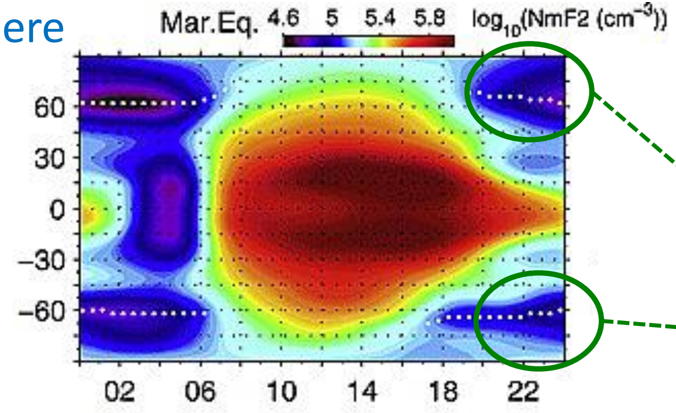

(He et al., 2011)

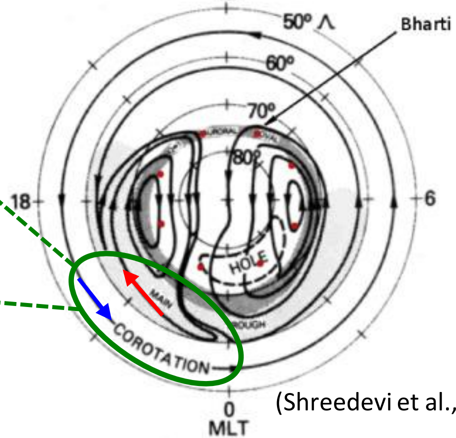

(Shreedevi et al., 2019)

- stagnation zone moves to lower latitude → MIT formed at lower latitude

SAPS and MIT (storm time dynamics)

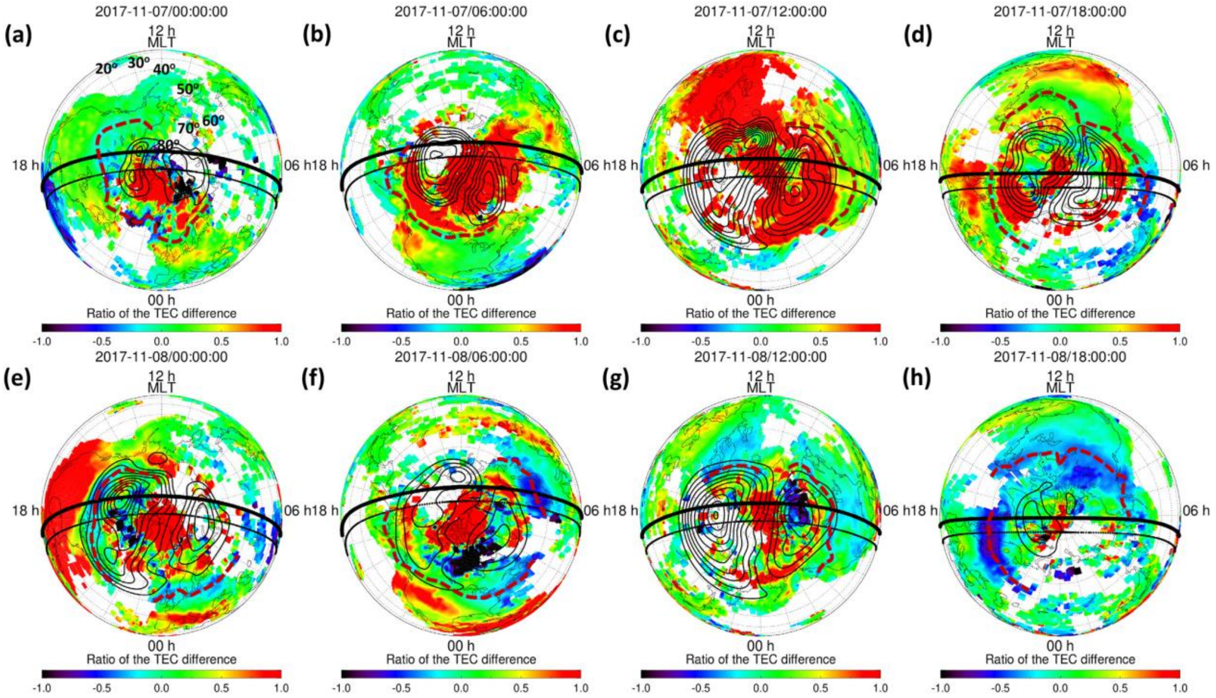

(Shinbori et al., 2021)

Normalised TEC:

rTEC = (TEC-<TEC>)/<TEC>

--- MIT (equatorward of the convection cells)

Storm enhanced density (SED) equatorward of MIT plots c) d) e)

- main phase: b) c) d) e)
- recovery phase: f) g) h)

Combined ground GNSS TEC, and SuperDARN electric potential maps,

MIT ~ SAPS

The Midlatitide (or Main) Ionospheric Trough (MIT)
LT dependence

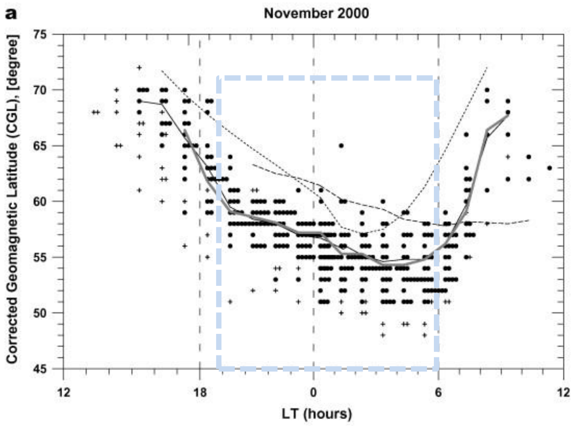

MIT latitude vs. LT
Ground-based TEC, N hemisphere

(Krankowski et al., 2009)

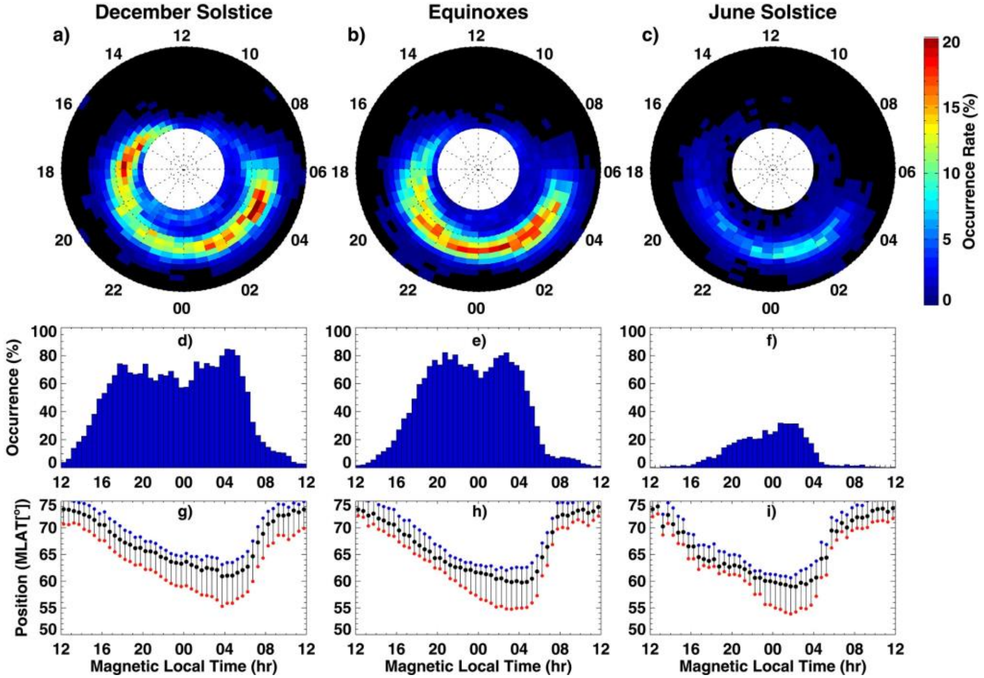

MIT latitude vs. MLT
Ground-based TEC, N hemisphere (Aa et al., 2020)

- merges into the cusp post-noon (stagnation model does not explain)
- lowest mlat in the post-midnight sector

The MLT dependence of the position of the Midlatitide (or Main) Ionospheric Trough (MIT) and SAPS

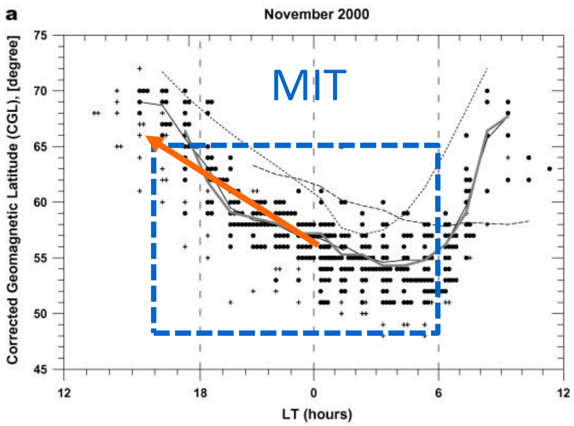

(Krankowski et al., 2009)

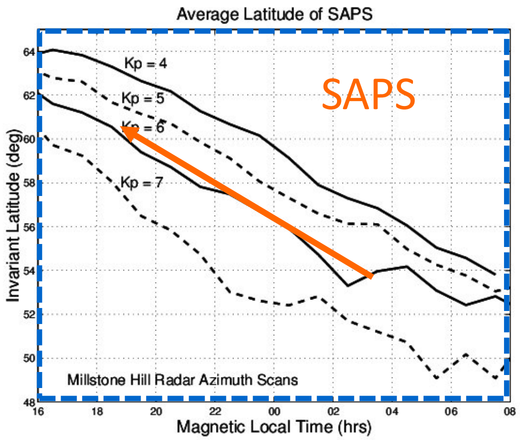

(Foster and Vo, 2002)

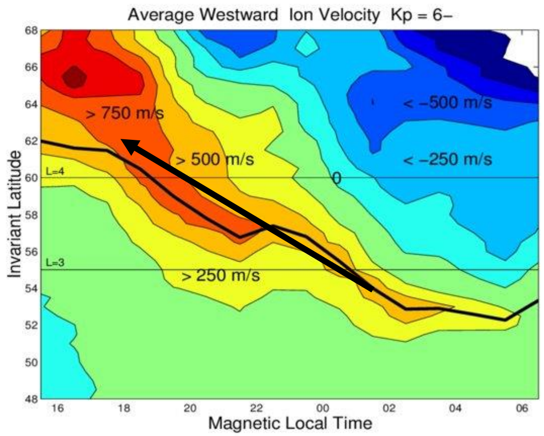

(Foster and Vo, 2002)

Similar MLT dependence: MIT extends toward afternoon MLT by SAPS (westward drift!)
plasma transport
westward drift ← polewaed E-field (SAPS E-field)

How the SAPS E-field is generated?
M-I-M feedback

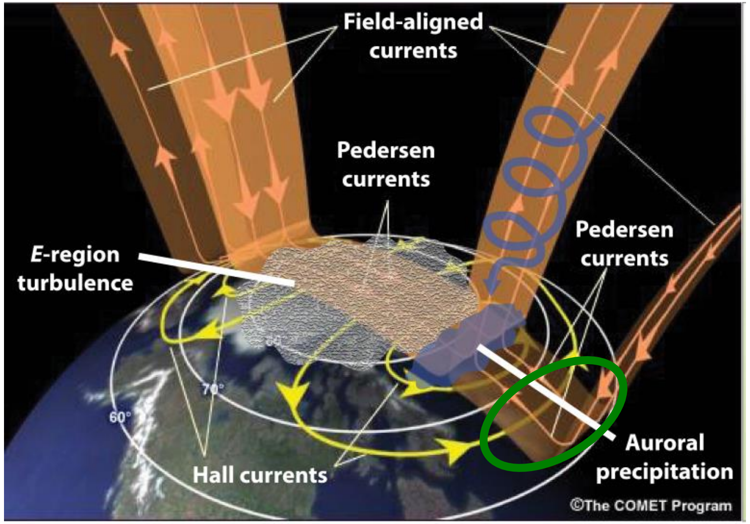

FACs of various origin are closed by ionospheric (Pedersen) currents

Ring Current

↓

$\mathbf{j}_{||}$ (R2 FAC ↓)
(sub-auroral zone)
Return current (R1 FAC ↑)

↓

closed in the ionosphere by
Pedersen currents
through a **conductivity contrast** ← auroral zone: high Σ_P; sub-auroral zone: low Σ_P

auroral precipitation

↓

large polaward **E** ← $\mathbf{E} = \mathbf{J}_P / \Sigma_P$

↓

E x **B** drift (SAID or SAPS)

↓

potential pattern
modified

MIT - SAPS

Horizontal drift (SAPS - blue)

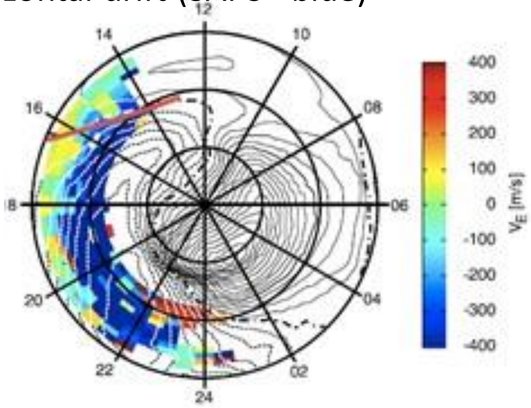

Ne (MIT: blue)

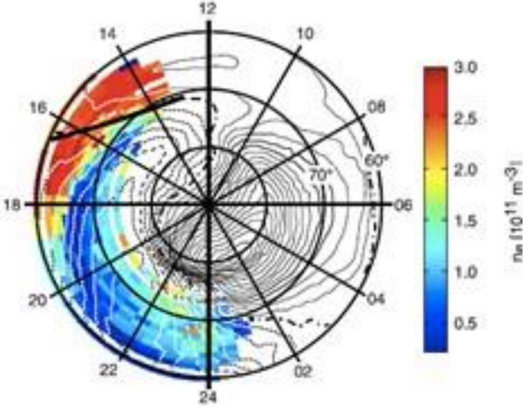

(Voiculescu et al., 2010)

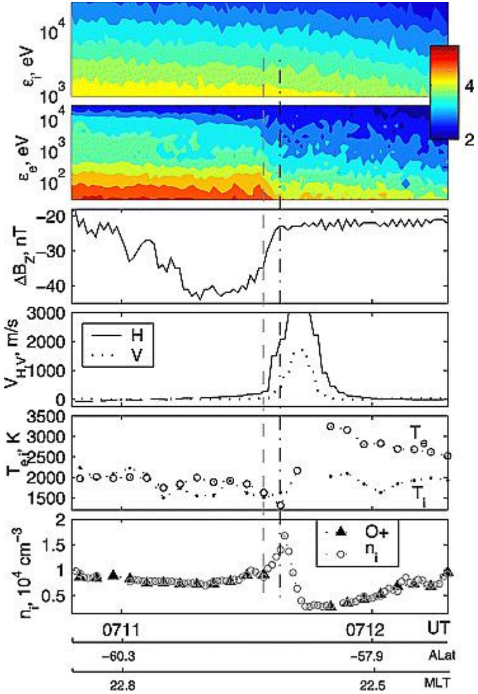

(Puhl-Quinn et al., 2007)

Similar MLT dependence: MIT extends toward afternoon MLT by SAPS (westward drift!)

„MLT evolution” of MIT? No

westward drift ← polewaed E-field (SAPS E-field)

SAPS: LEO observations of SAPS and MIT

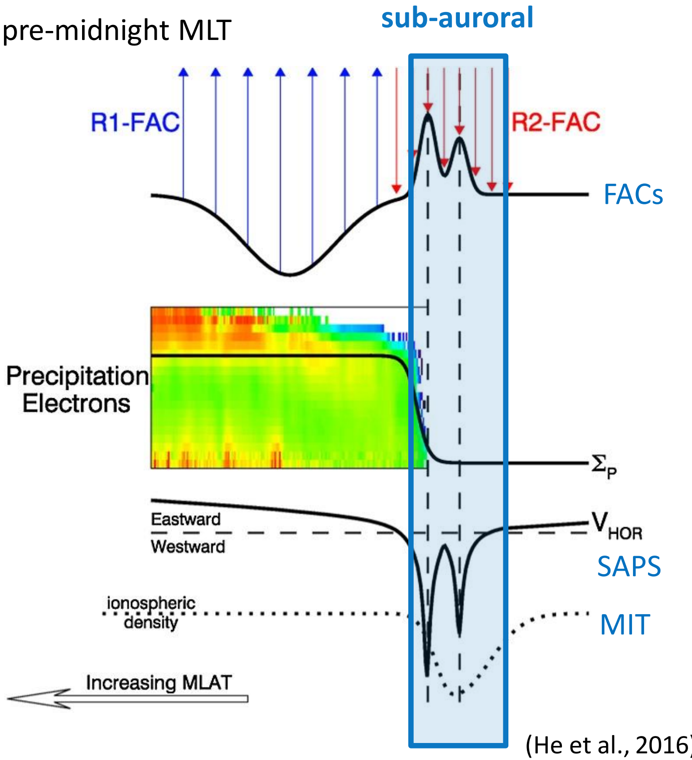

(He et al., 2016)

Relation of FACs, precipitation, conductance, SAPS and MIT

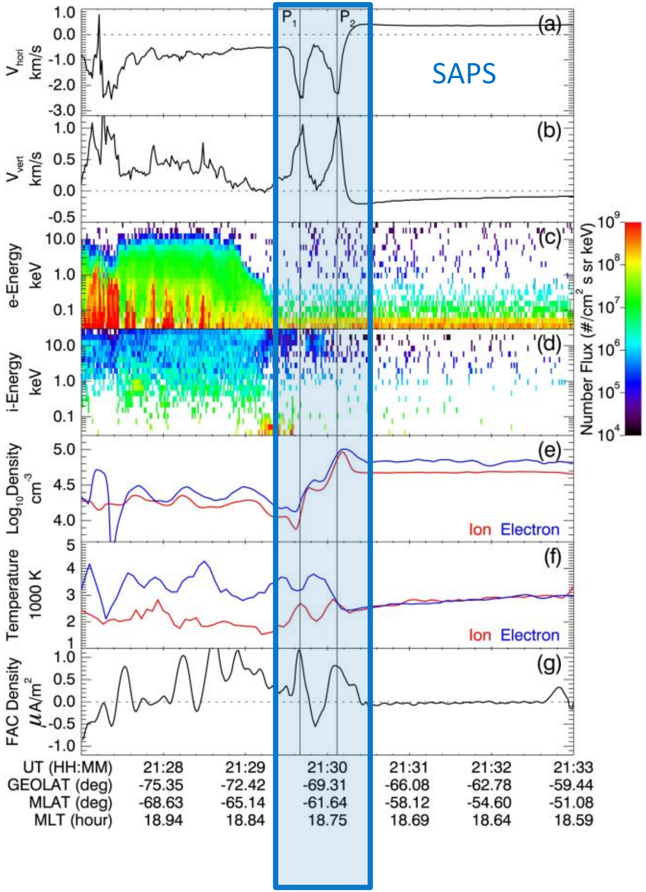

A **double SAPS** event observed by DMSP F13

(a) eastward horizontal drift velocity

(b) upward vertical drift velocity

(c) precipitating electrons and

(d) Ions

(e) ion/electron (red/blue) log densities,

(f) the ion/electron (red/blue) temperatures, and

(g) downward FAC density

(He et al., 2016)

SAPS in the magnetosphere

SAPS field mapping

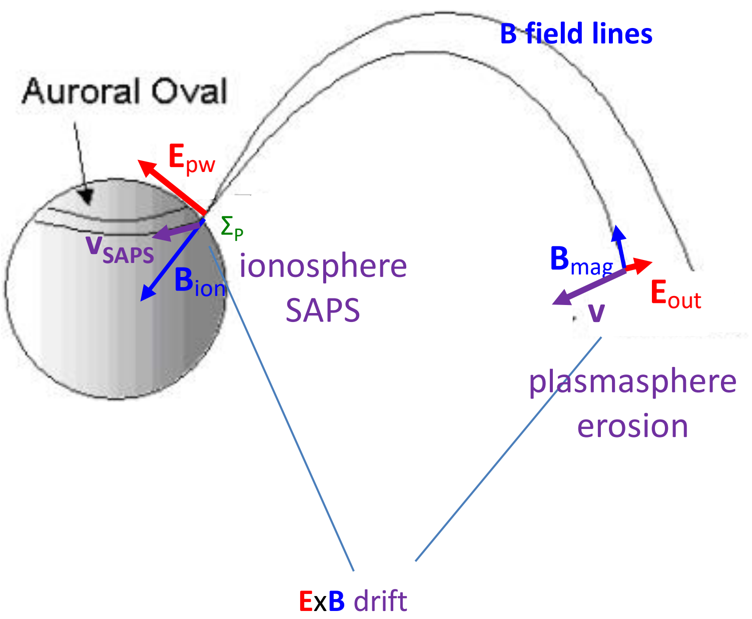

SAPS E-field

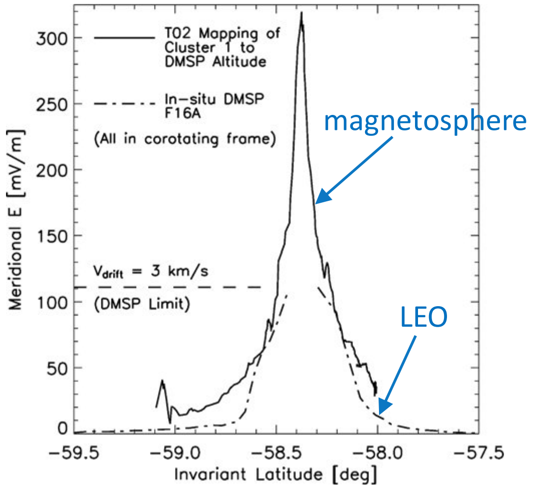

Mapping of Cluster 1 electric field to DMSP altitude (solid line) and in situ DMSP F16A electric field (dash-dot line) as functions of invariant latitude (Puhl-Quinn et al., 2007)

SAPS in the magnetosphere (corotation + convection + SAPS)

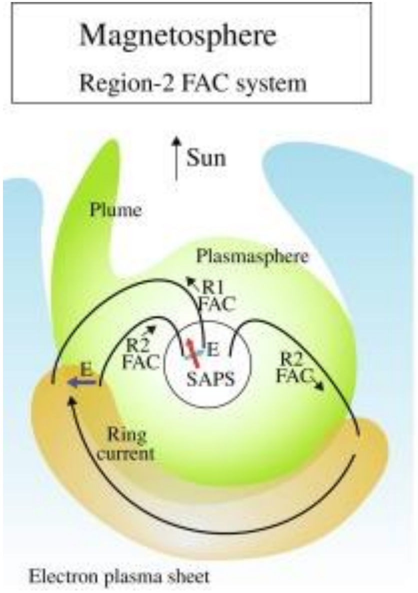

(Nishimura et al., 2022)

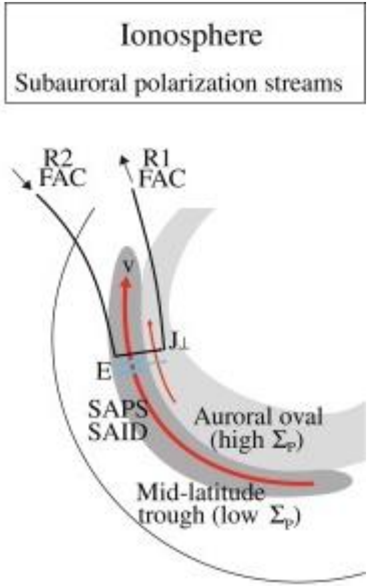

Equipotential contours (drift paths)

w/o ionospheric feedback | with ionospheric feedback

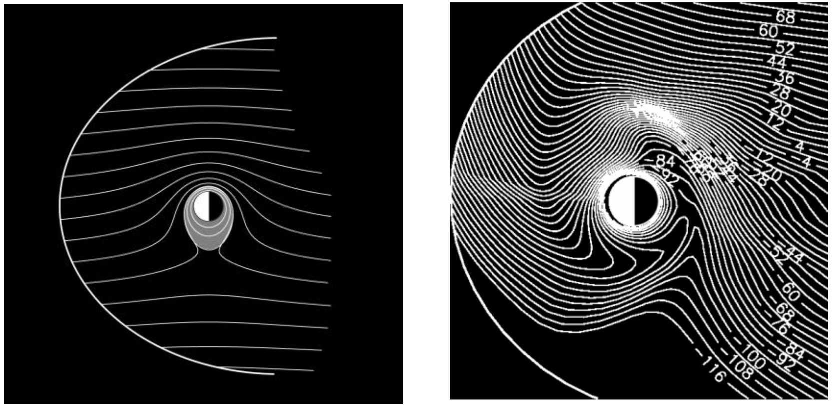

E field is modified ➔ convection pattern modified

(credit Y. Zheng)

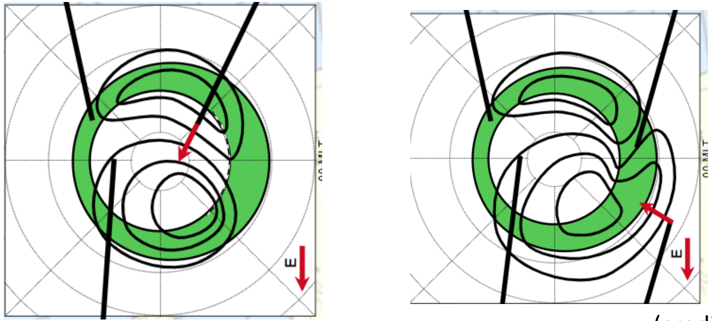

(credit A. Grocott)

SAPS: formation of drainage plumes

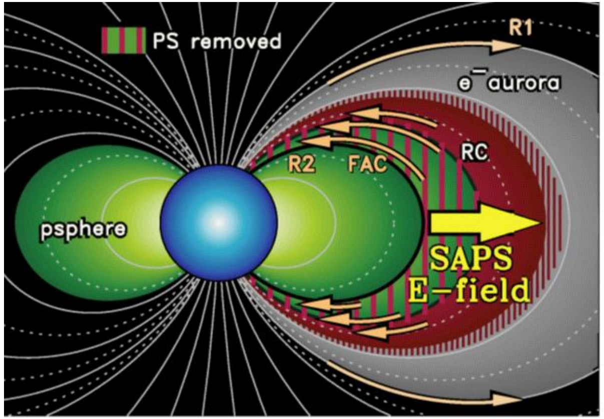

(credit: J. Goldstein)

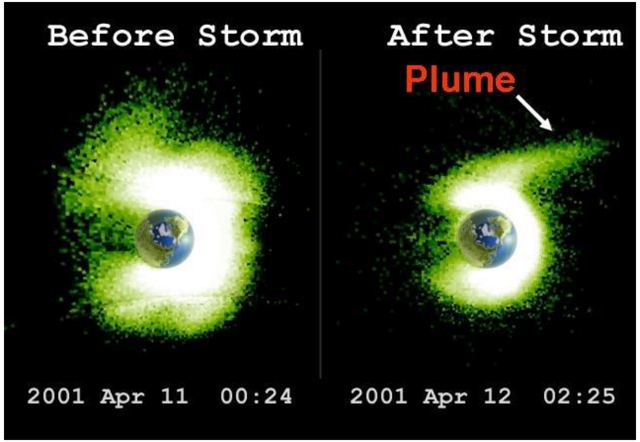

(NASA IMAGE EUV observations, credit: J. Goldstein)

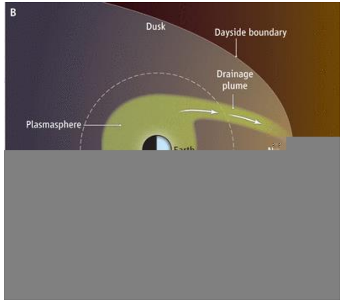

(Borovsky., 2014)

formation of plumes / role of SAPS

SAPS E field

↓

drives enhanced Sunward flow in the magnetosphere (transport the plasma of the bulge or the outer core plasma)

SAPS: formation of drainage plumes

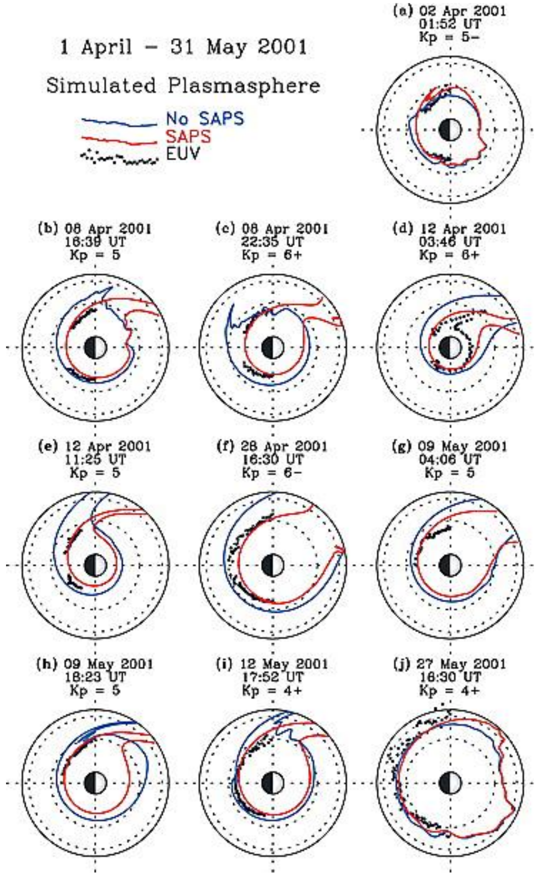

(Goldstein et al., 2005)

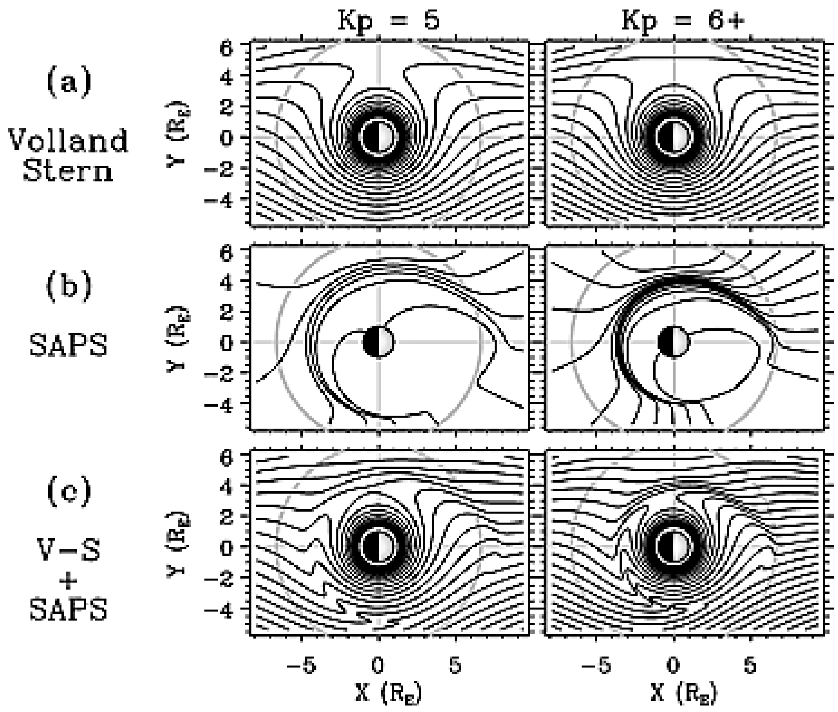

(Goldstein et al., 2005)

SAPS E-field is an important contribution and it is a result of from M-I coupling

SAPS: LEO observations of SAPS and MIT

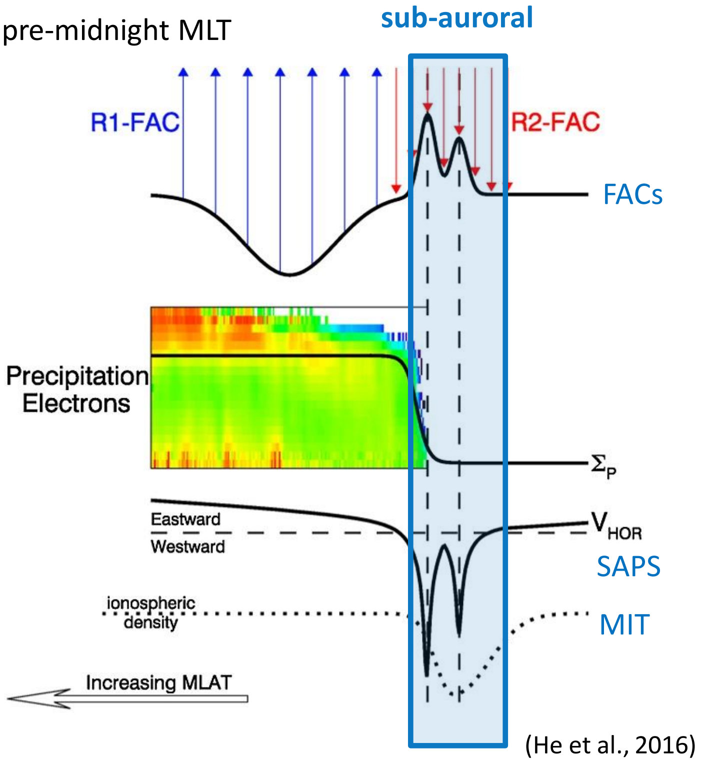

(He et al., 2016)

Relation of FACs, precipitation, conductance, SAPS and MIT

SAPS: enhanced westward flow in the ionosphere

↓

transports depleted plasma of the stagnation zone westward (earlier MLT) (**MIT**)

↓

frictional heating (**SETE**)

↓

enhanced recombination

↓

reduced conductivity (reduced cooling: **SETE**)

↓

deepens trough (**MIT**)

↓

increased SAPS

SAPS: SED and plasmaspheric plume mapping

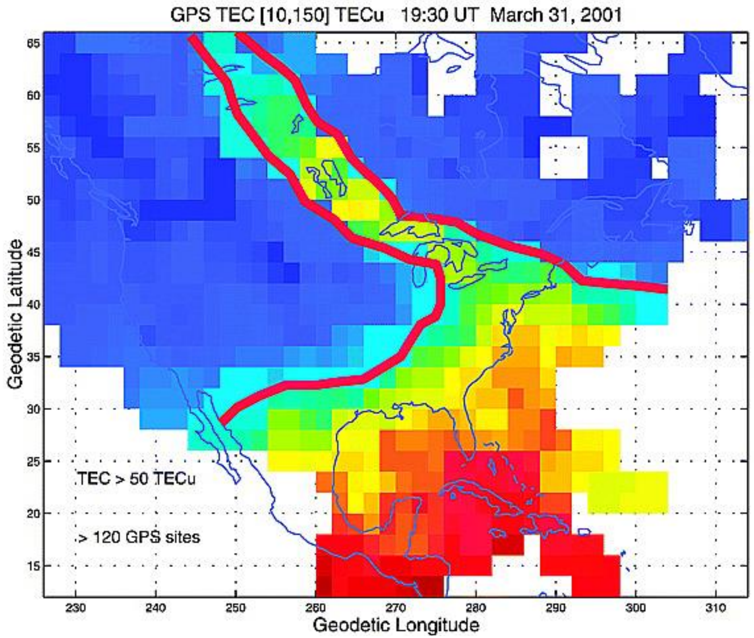

(Foster et al., 2002)

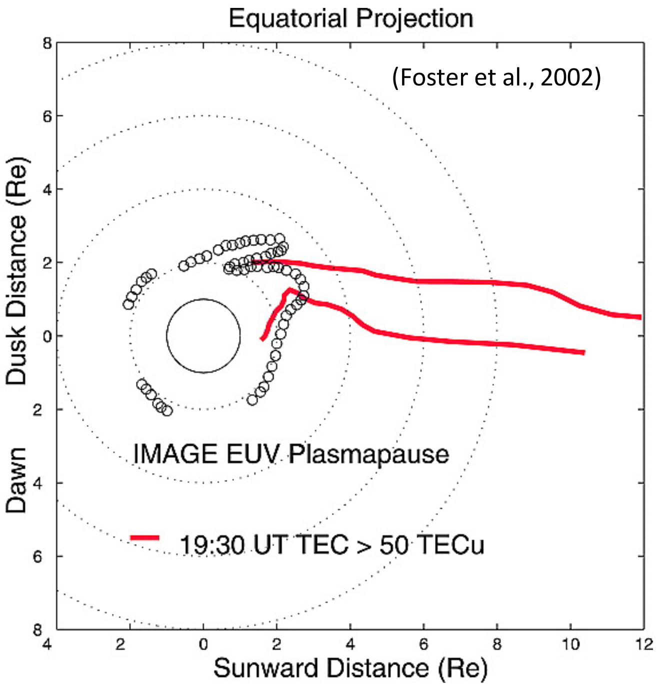

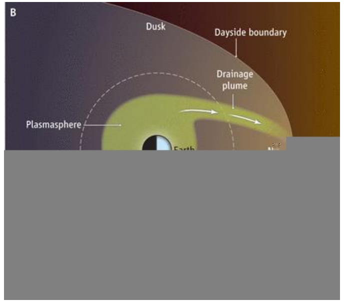

(Borovsky., 2014)

Storm enhanced density (SED) and Tongue of Ionization (TOI) found in GNSS TEC snapshot

GNSS TEC SED plumes map directly to the plasmaspheric erosion plume (Foster et al., 2002)

➔ Both flow channels are driven by SAPS E-field
(in this case the SAPS transported enhanced plasma)

SAPS: SED or MIT

Plume – SED (TOI) conjugation (enhanced plasma)

SAPS has a role also in forming MIT (depleted plasma)

Which then: MIT or SED/TOI?

SAPS is a plasma transport process (ExB drift, does not depend on density). SAPS transports any plasma population it crosses.

In the magnetosphere: bulge/core plasma → plume
In the ionosphere: depleted or enhanced plasma → MIT or SED/TOI

Observations of the plasmapause related ionospheric phenomena (MIT)

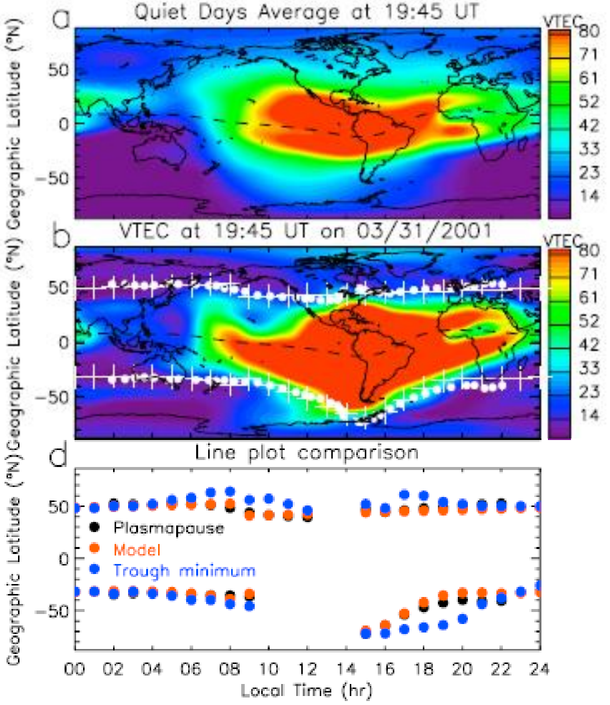

(Yizengaw et al., 2005)

MIT from global GNSS TEC maps
Quiet Days Average (at 19:45 UT)

2001.03.31 19:45 UT
(• - mapped PP, + - MIT model)
PP is from IMAGE EUV
Λ_{MIT} = 65.2° - 2.1Kp – 0.5 LT_0
(Moffett and Quegan, 1983)

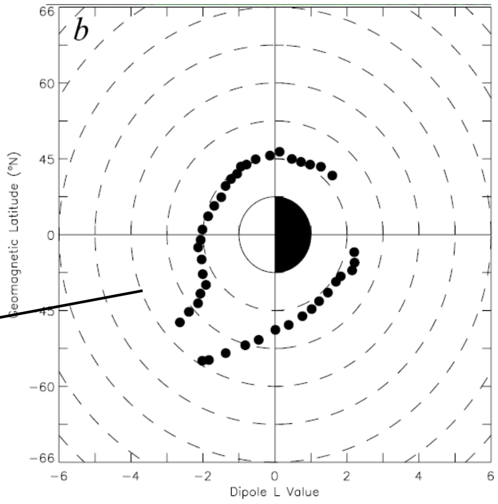

(Yizengaw et al., 2005)

Comparison of observations
(• - mapped PP, • - MIT model, (• - MIT observed)

Better agreement between PP and model MIT (in this case)
PP is near the ew edge of MIT (especially daytime) and **at all LTs**!

Height dependence of MIT-profile (Grebowsky et al., 2009)

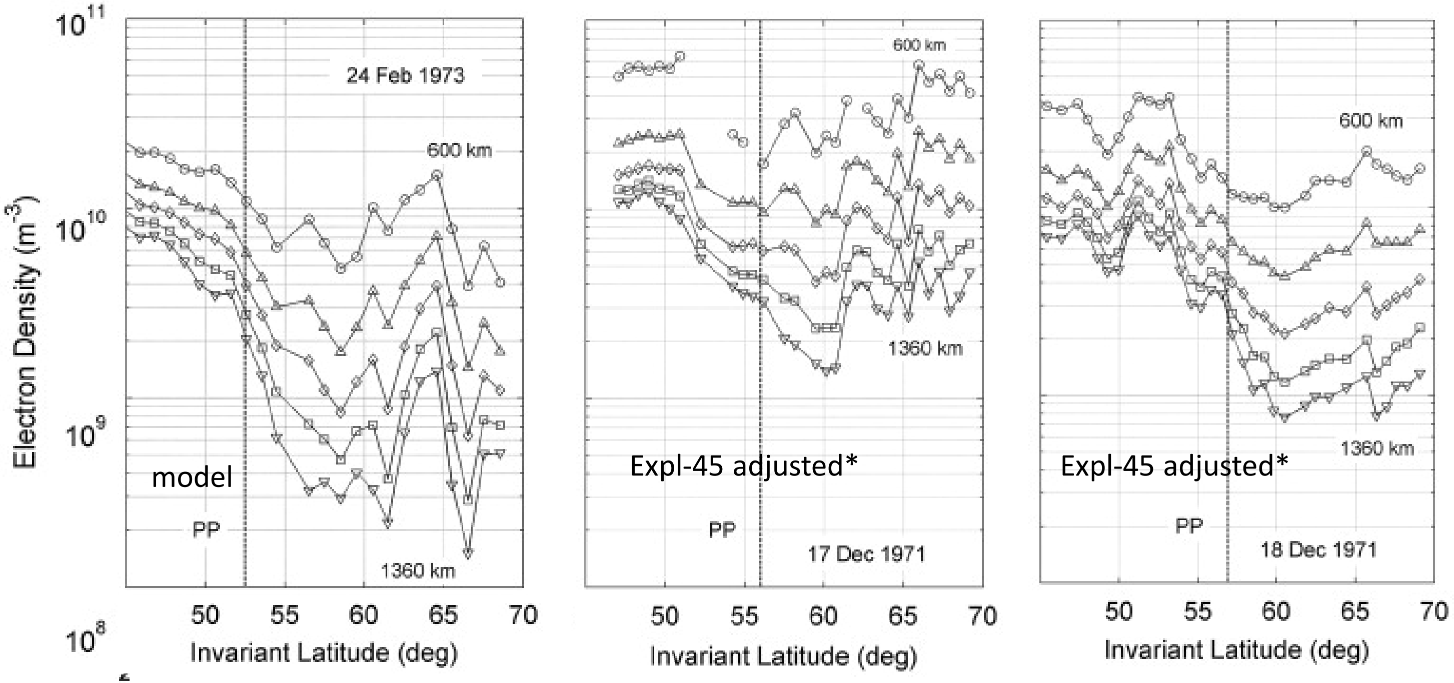

Height dependent PP-MIT relation

due to changing ion composition (O+/H+)

stant-altitude profiles of Ne derived from topside-sounder observations of ISIS-2 Ne(h) profiles

PP: Explorer-45 (E-field saturation) (CA1992 model for first plot)

* -0.25 based on T96 model (by the authors)

Height depndence of MIT-profile (Grebowsky et al., 2009)

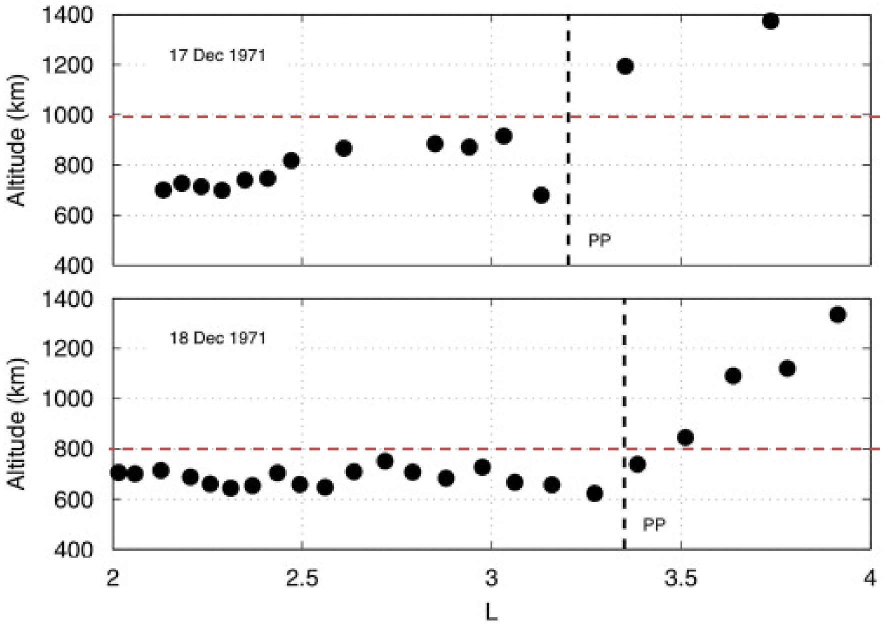

O+/H+ transition height is from model calculation from Ne(h) profiles assuming diffusive equilibrium (based on Webb et al., 2006)

O+/H+ transition heights along the ISIS-2 orbital tracks with the Explore 45 determined PP field lines

The Midlatitide (or Main) Ionospheric Trough (MIT) longitudinal variation

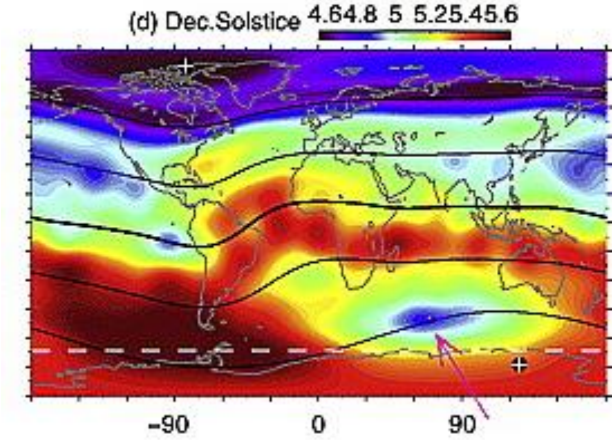

NmF2 map for December (He et al., 2011)

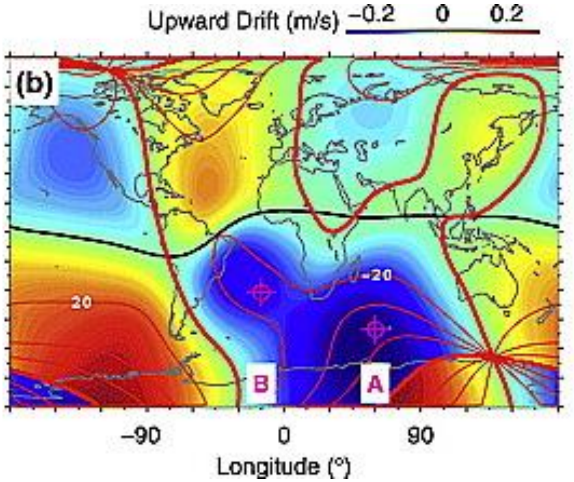

Upward drift corresponding to 1 m/s westward neutral wind (He et al., 2011)

Southern hemisphere: upward drift → higher hmF2 → less recombination → higher NmF2

sign of vertical drift depends on the sign of magnetic declinatio and the hemisphere

Generation of SAR arcs

RC – plasmasphere overlap

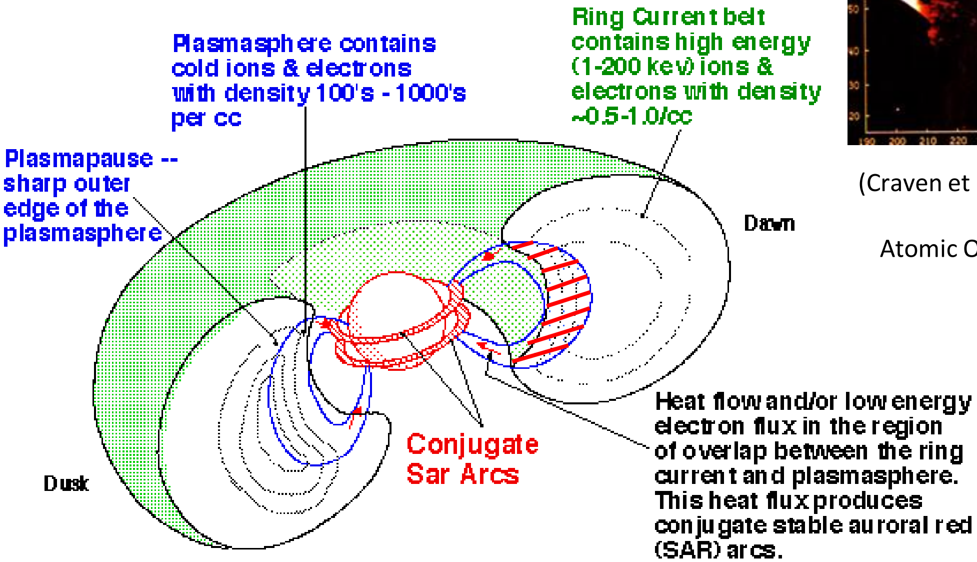

(credit J. Kozyra)

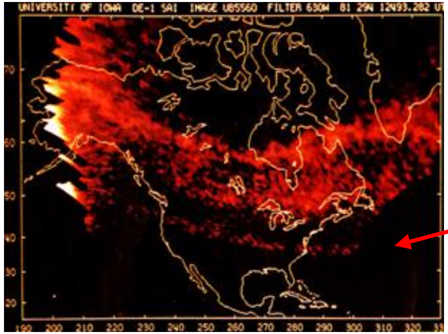

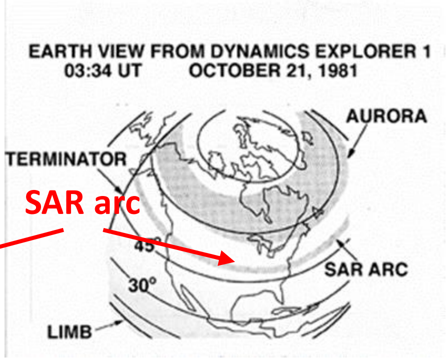

(Craven et al, 1982) DE 1 observation

Atomic O, excited d1 level (2 eV ← Te > 3000 K), emission at 630 nm. alt. Range: 200-

Magnetospheric sources of heat:

- Coulomb collisions (RC ions, cold electrons), mainly 30-50 keV O+ ions (Kozyra et al., 1997)
- Landau damping of EMIC waves (generated locally at the PP) (Cornwall et al., 1971)
- damping of kinetic Alfvén waves (Kozyra et al., 1997)

Ionosphere: heat is distributed among less particle in the low density trough → higher Te (**SETE**)

Observations of the plasmapause related ionospheric phenomena (MIT) (Chen et al., 2018)

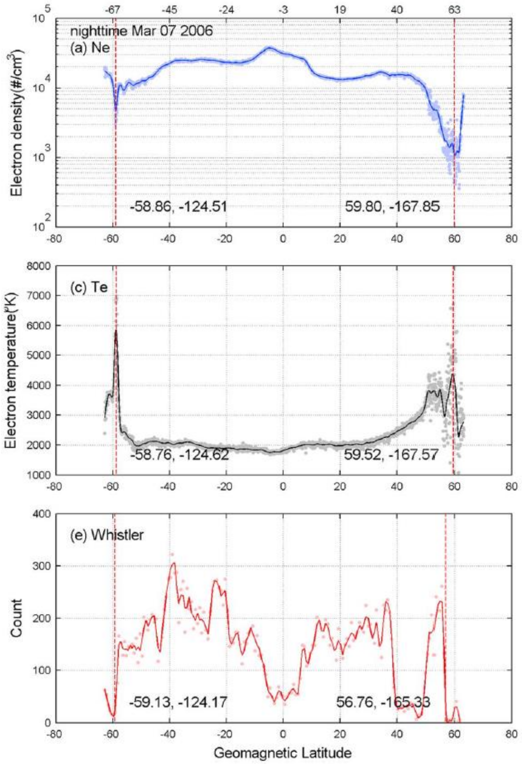

MIT minima

In-situ Langmuir probe Ne

DEMETER at LEO

2006-2009: # orbits: ~ 13,000

LT: ~22:30 (MLT: 19:00-01:00)

SETE (MIT associated Te peaks)

Langmuir Te

PW boundary of whistler occurrance

Close correspondence (on the nightside)

Observations of the plasmapause related ionospheric phenomena (MIT) (Chen et al., 2018)

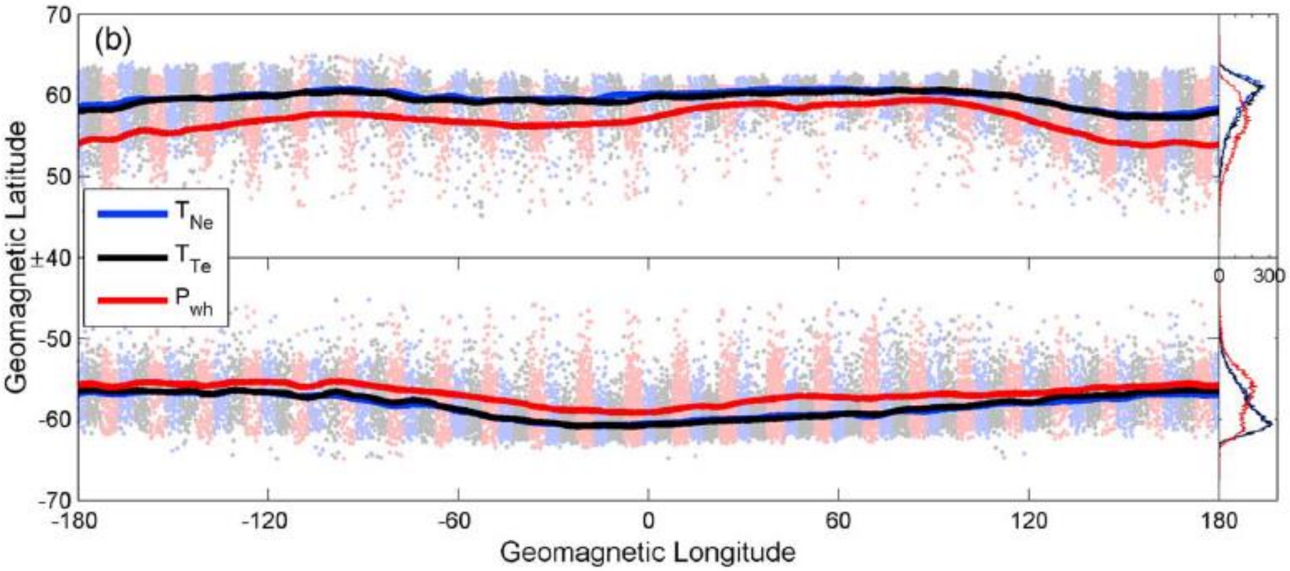

MIT minima

Te peaks (SETE)

PW boundary of whistler occurrance (WhB)

Outline

- Discovery of ionospheric phenomena and their relations to the plasmapause (a historical introduction)
- Phenomology of PP related ionospheric phenomena, their possible generation mechanisms in the light of M-I coupling
- **The use of LEO (Swarm) observations in monitoring plasmapause dynamics**

Motivation

Final goal: real-time specification of the plasmapause

Why at LEO?

- dynamic boundary, its location can change quickly (difficult to monitor with ground-based observations)
- polar LEO can provide **global coverage**, crosses all latitudes
- relatively high **cadence** of measurements: 64 PP footprint crossings daily (compared to magnetospheric satellites that provides 5-6 crossings daily)
- there are many LEO sats

Swarm observation of plasmapause related sub-auroral phenomena and dynamics

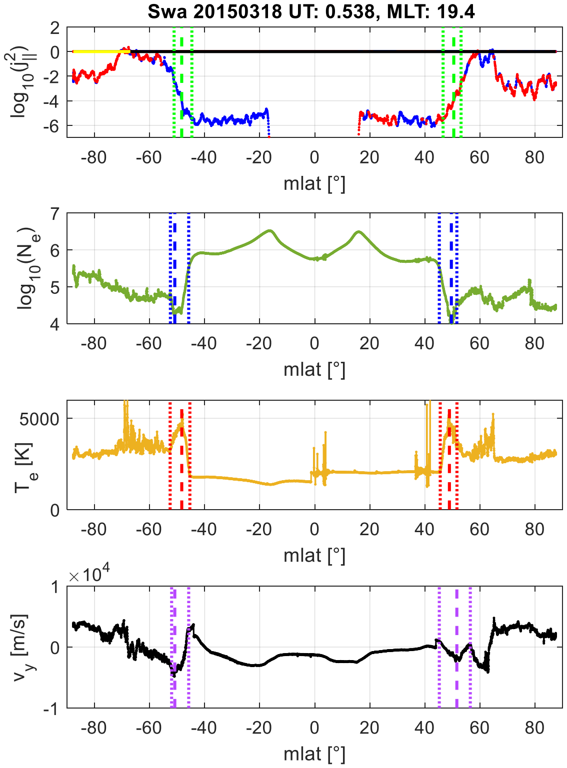

SSB
Small-scale FAC boundary
(Heilig and Lühr, 2013; 2018)

MIT
Mid-latitude Ionospheric Trough
(Heilig et al., 2022)

SETE
Sub-auroral Electron Temperature Enhancement
(Heilig et al., 2022)

SAID (SAPS)
Sub-auroral Ion Drift
Sub-auroral Polarisation Stream

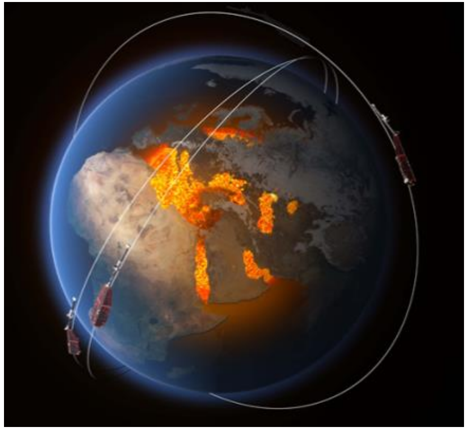

ESA's Swarm constellation
Swarm provides collocated and simultaneous observations of all of these boundaries

High inclination, polar LEO orbit
Orbital period : 91 min
altitude : 450-520 km
Slowly drifts in MLT

Plasmapause crossings (reference) data

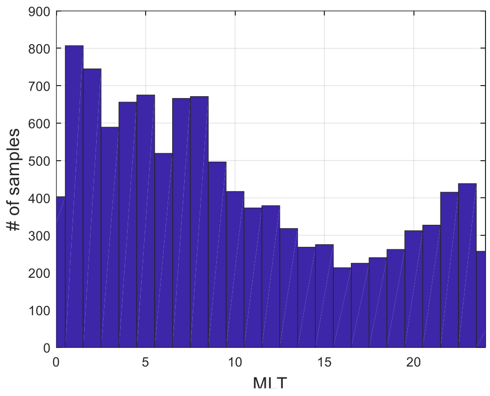

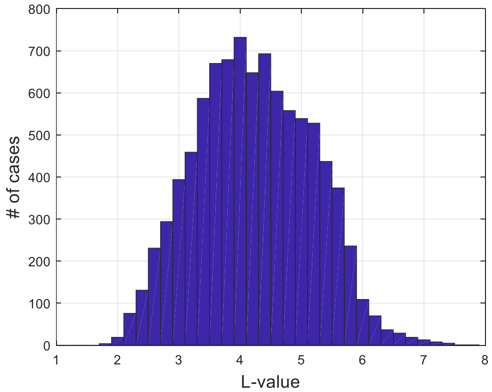

10946 PP crossings

2013-2017

- (THEMIS ESA amd EFI)
- RBSP EMFISIS
- Arase

Main features

- good MLT-coverage
- good L-coverage in [2; 6]

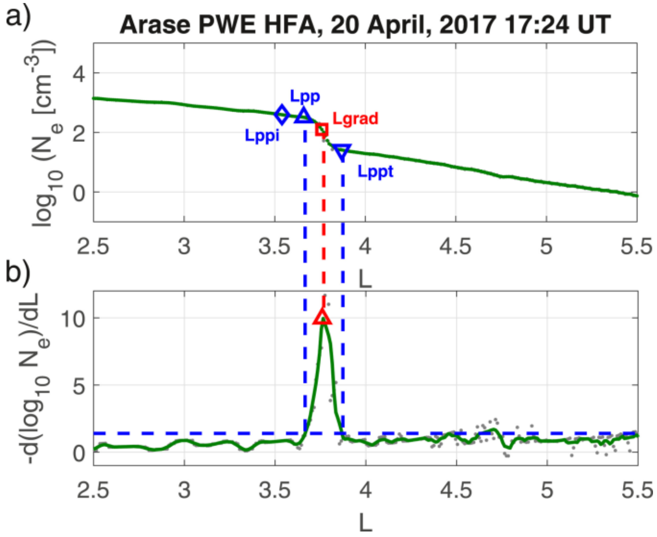

Arase PP crossing detection example. a) density profile; b) density gradient profile (Heilig et al., JGR, 2022)

Swarm products (DISC ITT 4.4 PRISM)

Swarm PRISM product package consists of two independent groups of L2 products available at https://earth.esa.int/eogateway/missions/swarm/data (as MIT and PPI)

MITx_LP_2F and **MITxTEC_2F:** location, size and shape of the **Mid-latitude Ionospheric Trough**

- based on Langmuir probe observations – EFIx_LP_1B
- based on GNSS TEC observations – TECxTMS_2F

Product identifier	**MITxTEC_2F**
Definition	Midlatitude Ionospheric Trough Boundaries and Minima from TEC
Inpu	
Inpu	
Spat	

Product identifier	**MITx_LP_2F**
Definition	Midlatitude Ionospheric Trough Boundaries and Minima
Input Data	EFIx_LP_1B[1], AUXxORBCNT
Input Time Span	24 h[2]
Spatial representation	One geographic and QD-latitude/longitude pair, the McIlwain L-value as well as radius for each output position at the nearest LP measurement for each trough crossing, i.e. four per orbit.

PPIxFAC_2F: equatorward boundary of SSFACs derived from FAC (FACxTMS_2F) and the associated **midnight Plasmapause index**

Product identifier	**PPIxFAC_2F**
Definition	Equatorward boundary of SSFACs and the associated midnight PP index
Input Data	FACxTMS_2F[1], AUXxORBCNT
Input Time Span	24 h[2]
Spatial representation	One geographic and QD-latitude/longitude pair, the McIlwain L-value as well as radius for each output position at the nearest FAC measurement for each trough crossing, i.e. four per orbit.

MIT

SETE

SSB

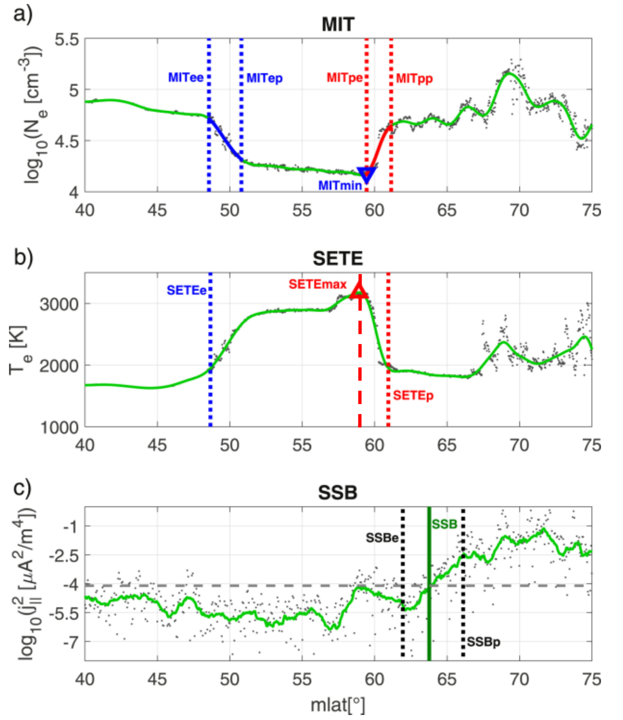

Midnight Plasmapause location proxy

We derive **MPP** (midnight PP location proxy)

- **MIT** observations made between MLT 22-06 are reduced to MLT midnight (linear MLT dependence)
- **SSB** observations made between MLT 22-06 are reduces to MLT midnight (SSB boundary model, Heilig et al., 2018)
- all reduced **MIT** and **SSB** values from the 3 Swarm satellites are **smoothed** (weighted* average)

Results: **MPP**: an **improved PP proxy based on LEO data only**

Current latency: 7 days due to limitations of the current downlink schedule and processing chain

(New: input data are available with a few hour latency)

* weights are defined based on the source of information (MIT or SSB, and the related product quality flags)

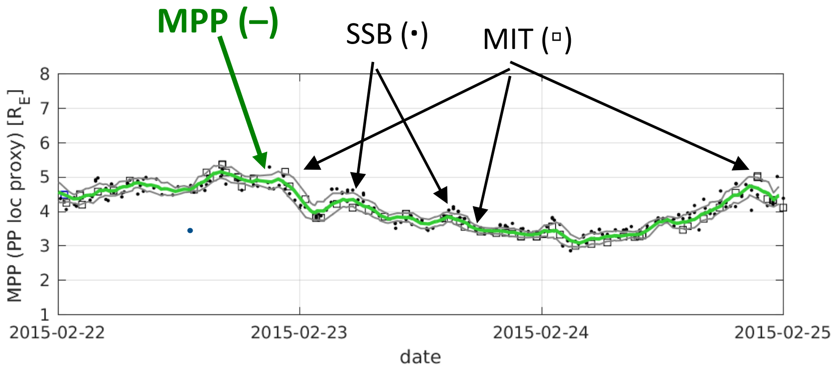

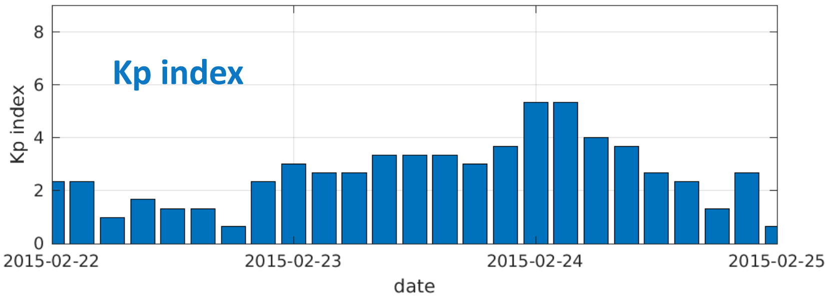

Comparison of in-situ RBSP post-midnight plasmapause and SSB: Swarm equatorward boundary of small-scale FACs

70-day comparison

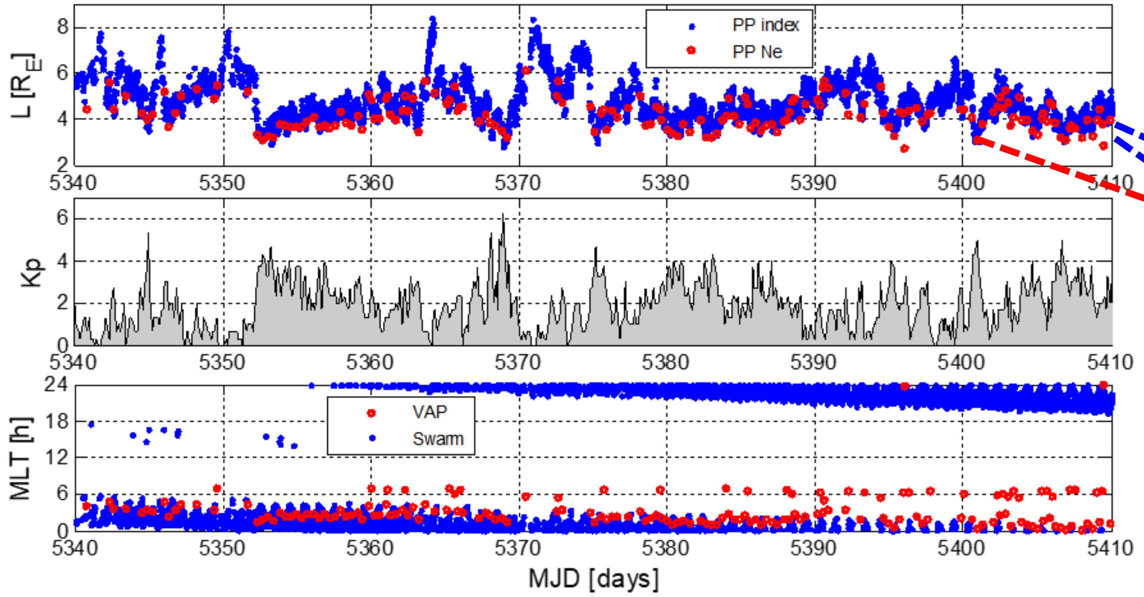

(Heilig and Lühr, 2018)

SSB positions are mapped into the magnetosphere along field lines for direct comparison with PP

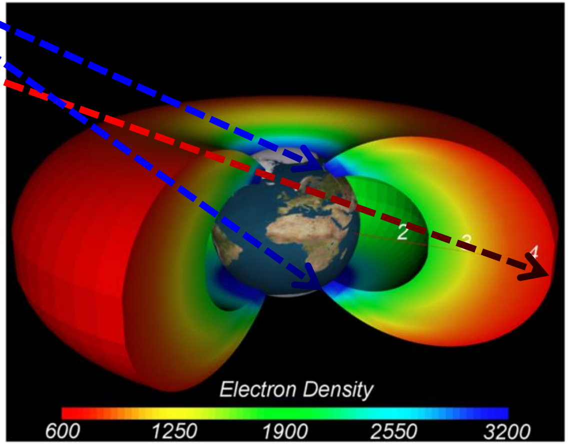

1) good correspondence:
SSB and **PP** lie along the same field lines
2) high sensitivity to Kp
3) higher cadance at LEO

Comparison of in-situ IMAGE RPI post-midnight PP and SSB: Swarm equatorward boundary of small-scale FACs

45-day comparison

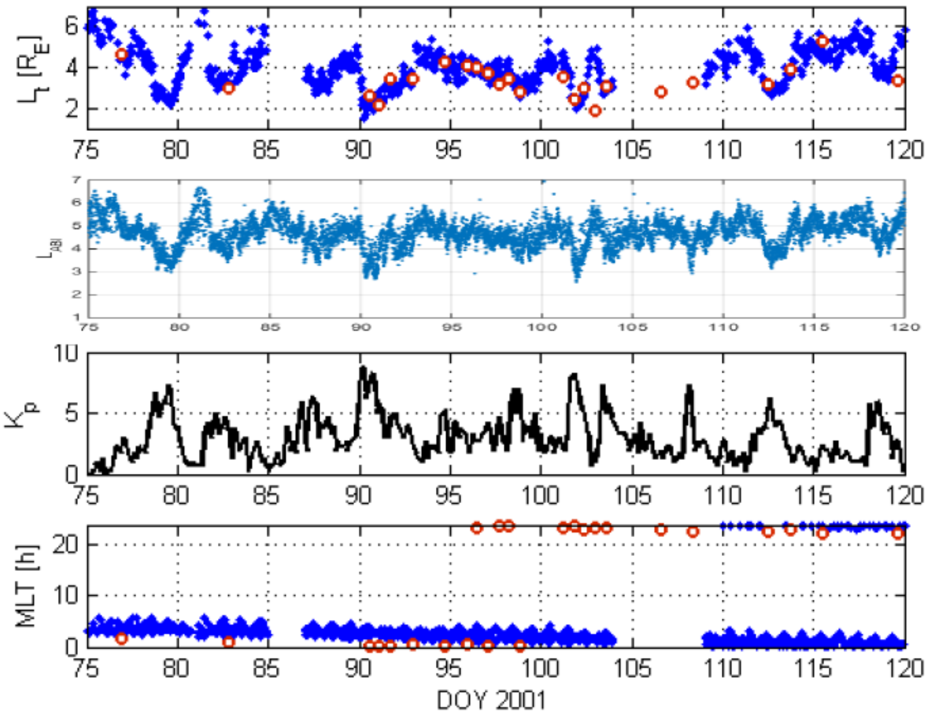

SSB (CHAMP) / **PP** (IMAGE RPI)

DMSP ABI
(precipitation boundary / auroral electrons)

Kp

SSB (PP) is closely related to ABI (during active times SSB is equatorward of ABI

MIT – Plasmapause: statistical comparison

Wide MLT interval of (statistical) coincidence
from the bulge (Kp-dependent) to dawn

Swarm ABC: 2014-2020
MIT: ~ # 63 000

RBSP, Arase, THEMIS: 2014-2017:
PP ~ # 11 000

MIT – Plasmapause: statistical comparison

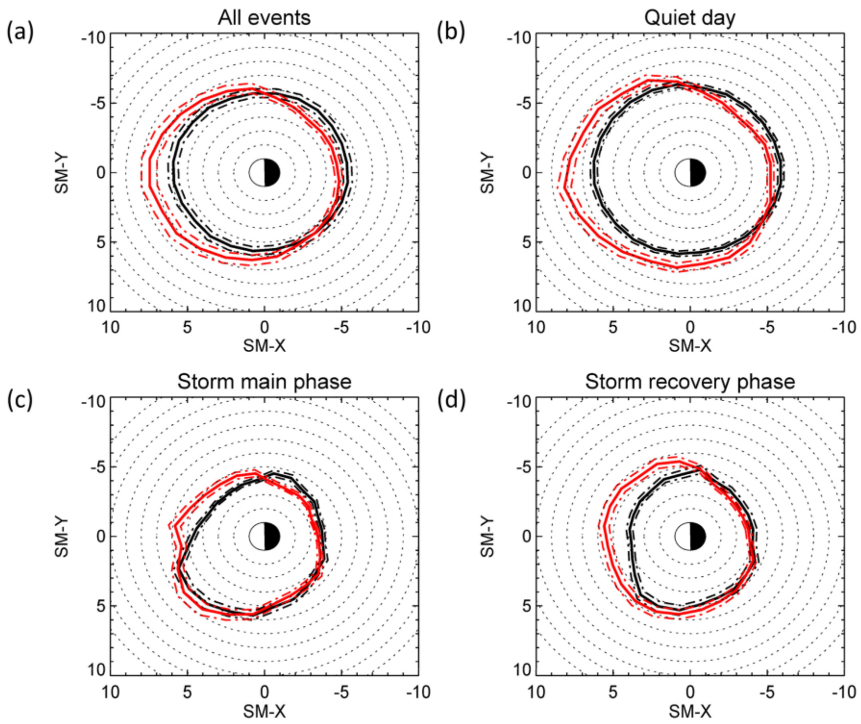

(Shinbori et al., 2021)

Different study!

Simultaneous PP and MIT

PP: in-situ Arase PP-crossings

MIT: from ground-based GNSS TEC maps (5-min, 2.5°x2.5°averaged, from 30 s cadence, 0.5°x 0.5° grid)

TEC

- height integrated
- derived from slant TEC (mapping functions)

MIT and plasmapause evolution

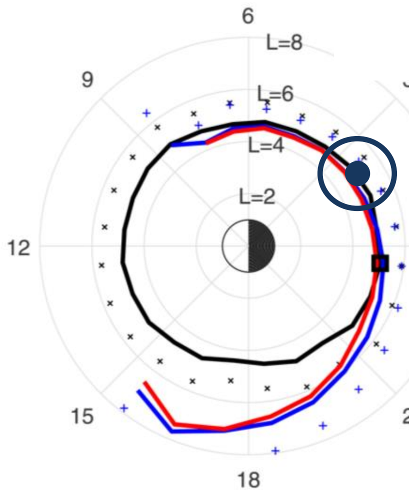

Nightside PP locations (open circle) gave the highest correlation with **simultaneous, co-located MIT** (dot) observations

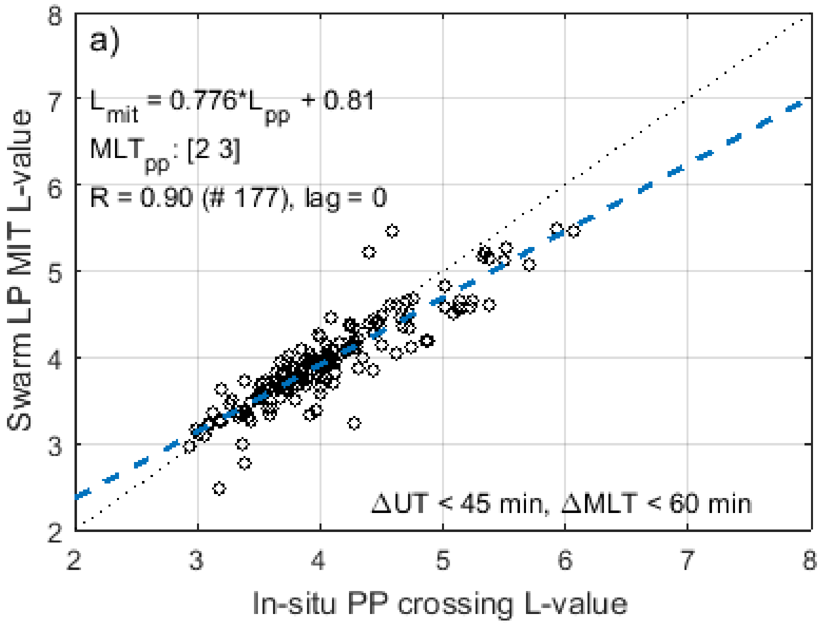

Simultaneous **MIT** vs. **PP** in the MLT sectors 2-3 h
r = 0.90, 0.96, 0.87 and 0.84

MIT and plasmapause evolution

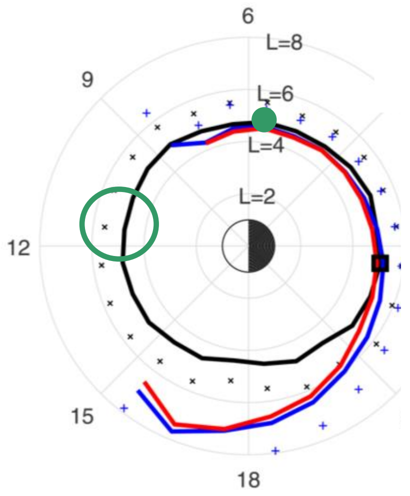

Dayside PP locations (open ci
at MLT 11.5 h gave the highes
correlation **with past** (5.5 h
earlier) **observations of MIT**
minima **at MLT ~6 h**

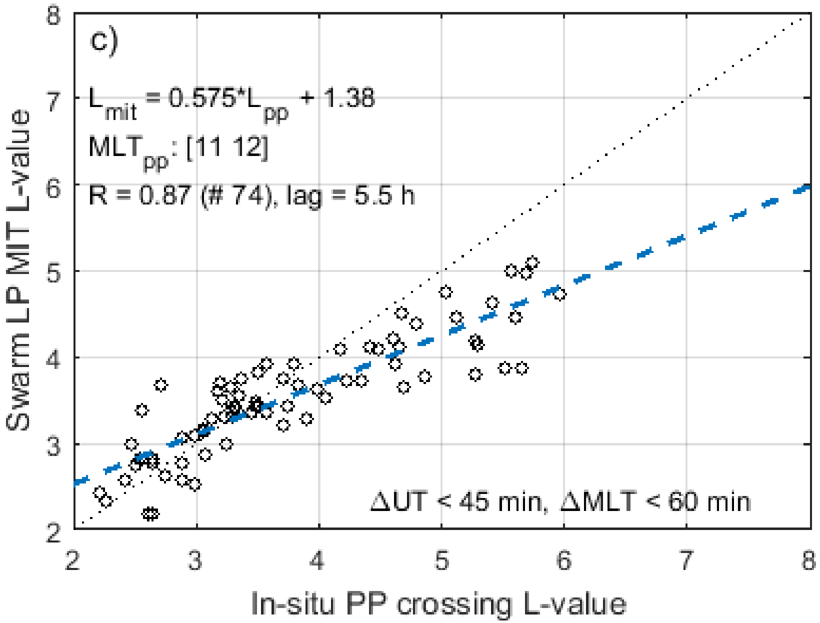

MIT vs. **PP** in the MLT sectors 11-12 h
r = 0.90, 0.96, 0.87 and 0.84

MIT – Plasmapause

Swarm ABC: 2014-2020
MIT: ~ # 63 000

RBSP, Arase, THEMIS: 2014-2017:
PP ~ # 11 000

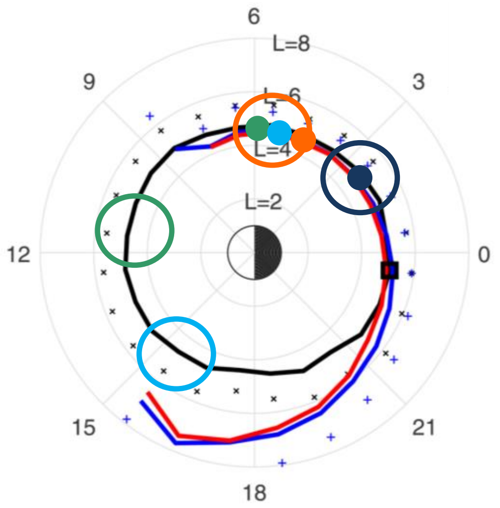

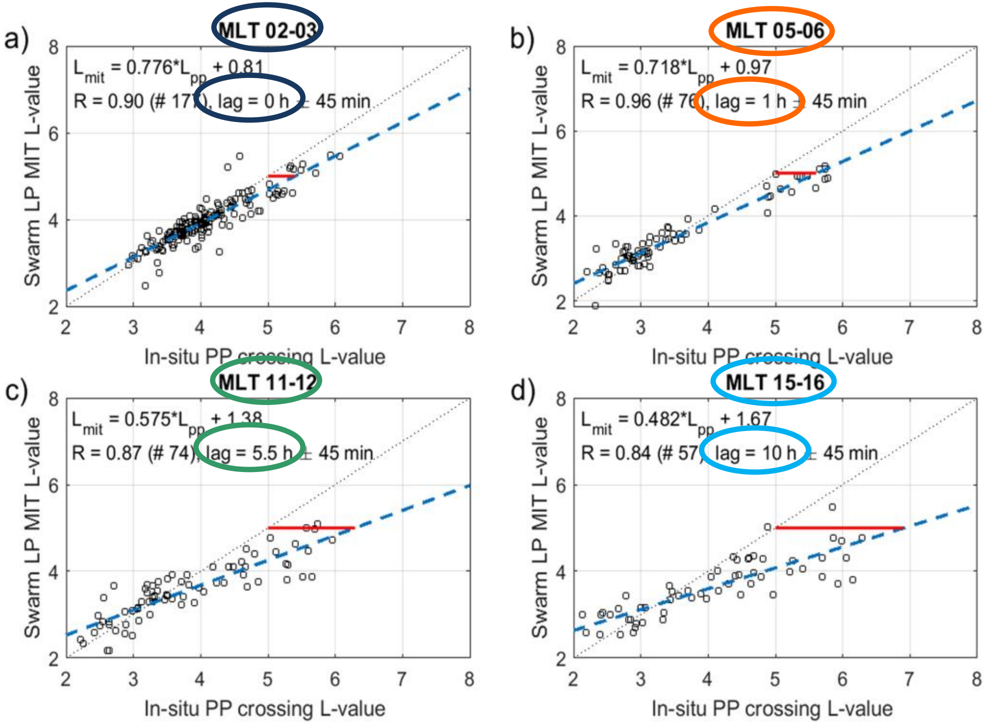

Dayside PP locations (open circle) gave the highest correlations with **past dawn (**MLT ~ 6 h) **MIT locations** (dots)

High correlation between MIT and PP on the night and dawn side
Dayside PP has highest correlation with night side MIT variation observed few hours earlier (Heilig et al., 2022)

MIT and plasmapause evolution

Varying correlation strength depending on MLT and time lag

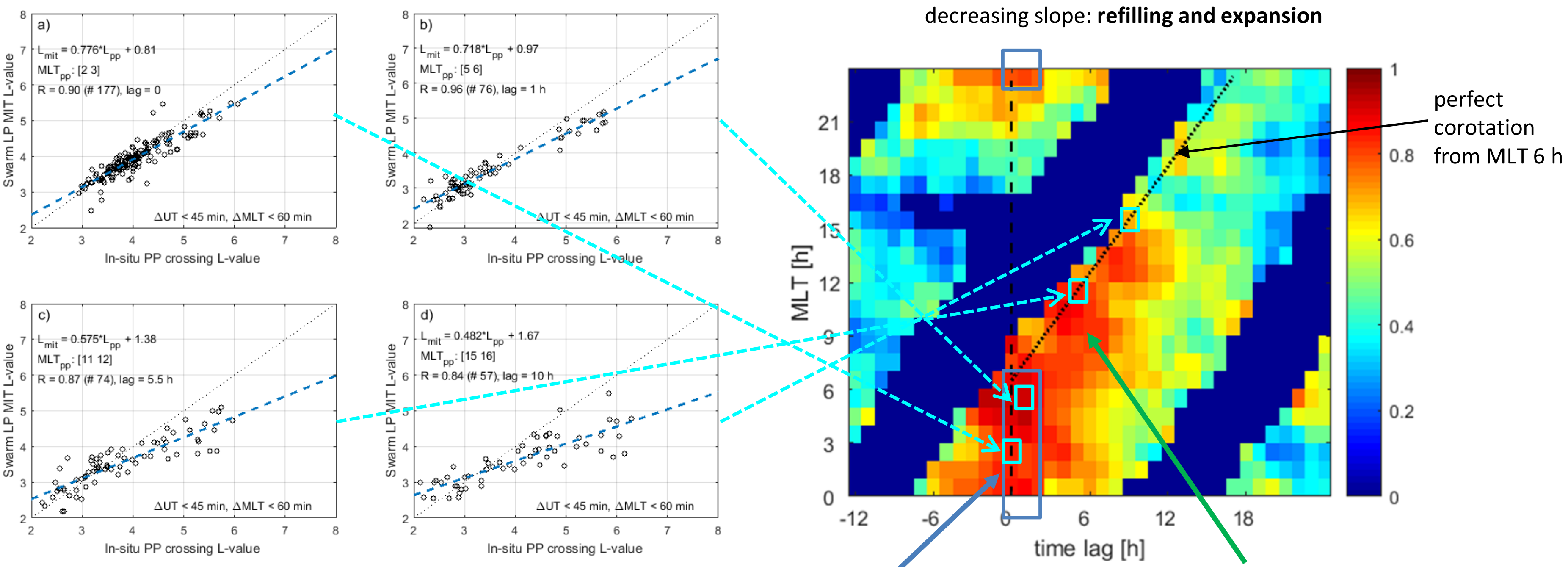

MIT vs. **PP** in the MLT sectors 2-3, 5-6, 11-12 and 15-16, respectively
cross-correlation maximises at **0, 1, 5.5, 10 h lag**, **respectively**
r = 0.90, 0.96, 0.87 and 0.84

fresh PP is formed here
(where lag is ~ 0 h)

PP appears at later MLTs (dayside) with **corotation** (PP formed earlier in the post-midnight sector)

MIT and plasmapause evolution

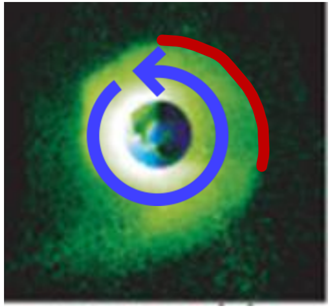

These results (MLT dependent response time) are in full agreement with the scenario that

- new PP is primarily **formed on the night side** (post-midnight MLT sector) (~ 0 response time) and
- propagates to the dayside by **co-rotation with the Earth** (and plasmasphere) (MLT - dependent response time)

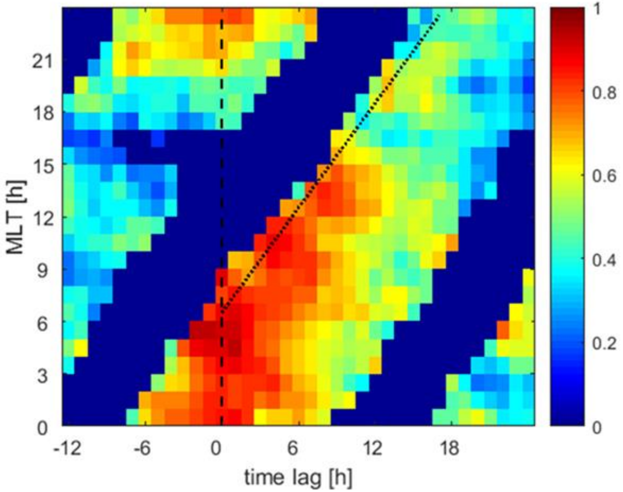

MIT-PP correlation as a function of MLT (vertical) and response time (horizontal axis)

Consequently

- MIT can be used as a proxy for the nightside PP position
- dayside PP positions can be recovered from the time history of nightside MIT and SSB

(Heilig et al., 2022)

Model architecture

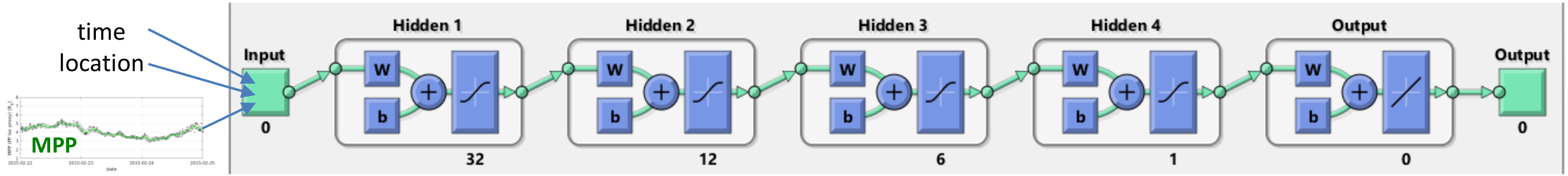

Multilayer feedforward network

Inputs:
- Time: DoY / UT
- Location: mag. latitude / MLT
- **3-day time history of MPP**

Training (83%), validation (12%) and test (5%) subsets

Target
- PP location from in-situ PP-crossings: # 8217

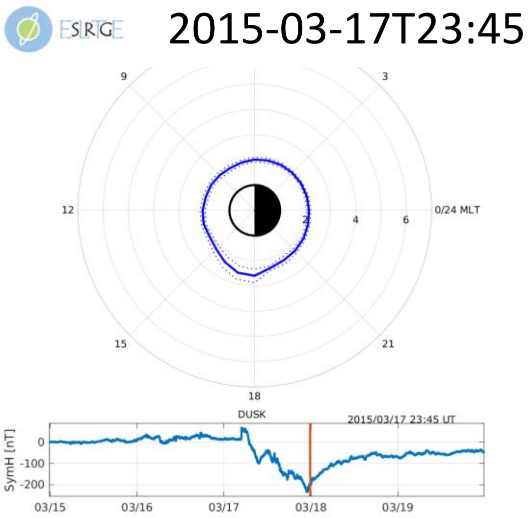

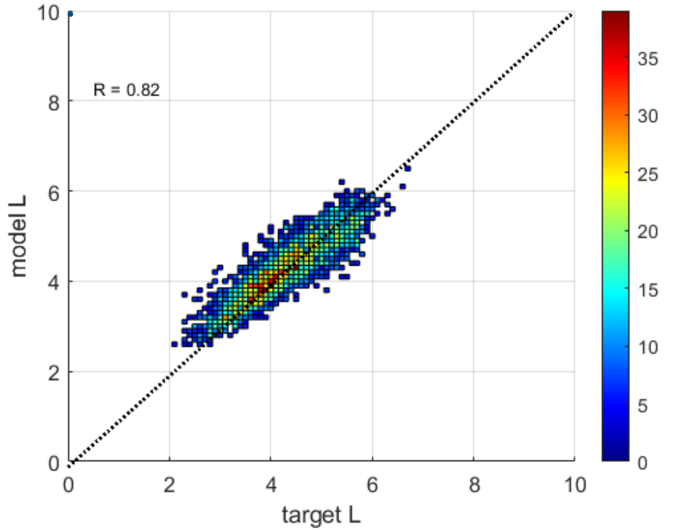

Empirical NN-based nowcast model

RMSE: **0.61**, R = **0.82**

This model

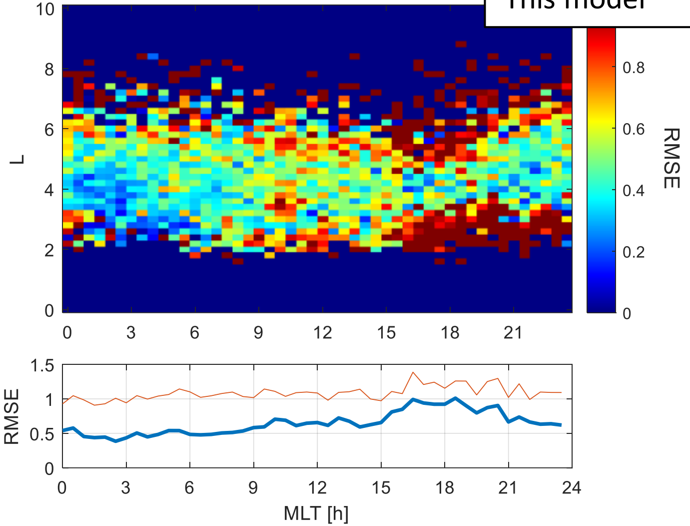

Inputs:

- Time: DoY / UT
- Location: mag. latitude / MLT
- **3-day time history of MPP**

Performs better than the one with magnetic indices, solar flux and solar wind parameters as input

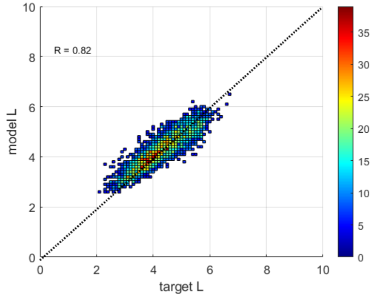

RMSE: 0.68, R = 0.76

PLASMA nowcast model

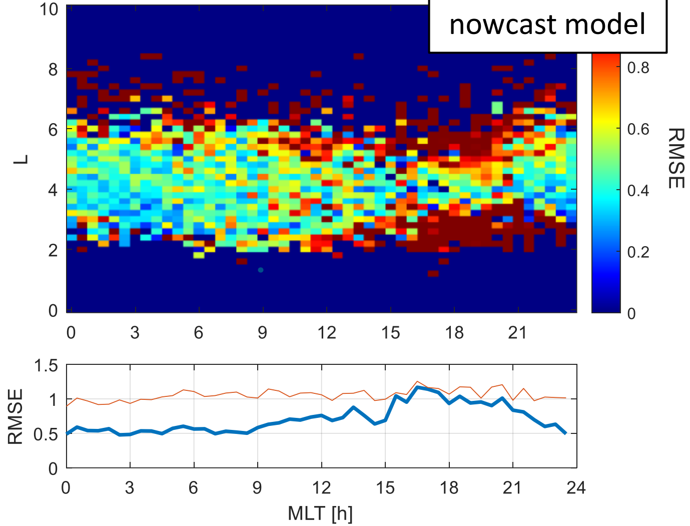

Inputs:

- Time: DoY / UT
- Location: mag. latitude / MLT
- **3-day time history of Dst**
- **3-day time history of Hp30**
- **3-day time history of f10.7**
- **3-day time history of solar wind speed**
- **3-day time history of IMF Bz**

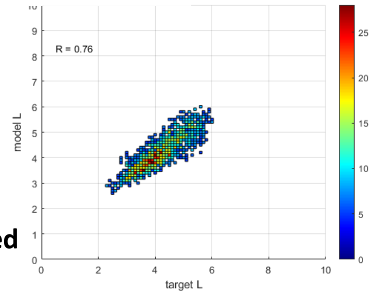

MIT and plasmaspheric plume mapping

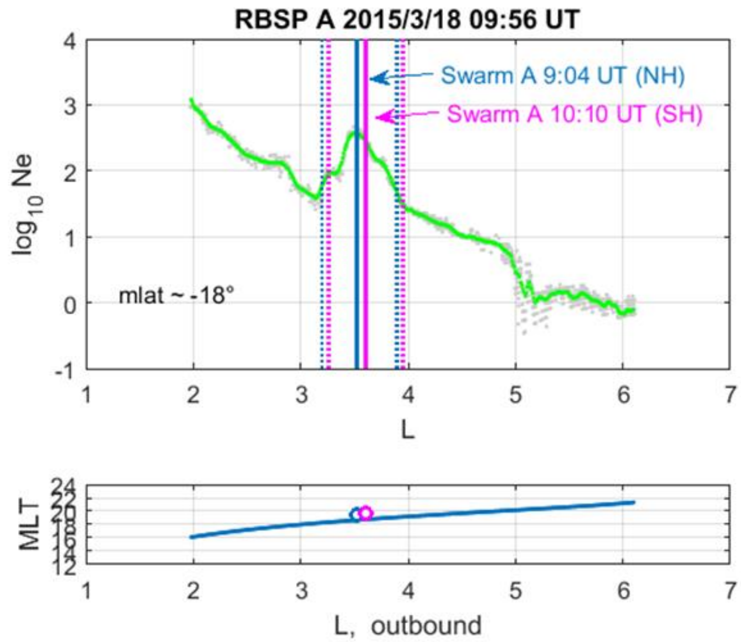

(top) RBSP A, 18 March, 2015 electron density (green) and MIT boundaries (dotted lines) and minima (vertical lines) observed by Swarm A, mapped onto the equator, (bottom) MLT of RPSP (solid line) and Swarm (circles) (Heilig et al., 2022).

Example: 2015 March storm

1. RBSP A – Swarm conjunction on 18 March
2. RBSP A observs a pume (green curve, increased density), while Swarm A crosses a MIT structure. (first observation of a plume-MIT conjunction)
3. (both are produced by the same SAPS E-field)

Can **MIT** observations be used to monitor plumes?

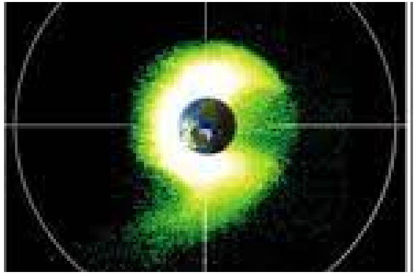

NASA IMAGE EUV, credit: J. Goldstein

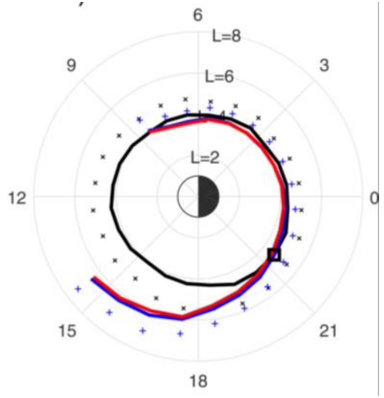

MIT and plasmaspheric plume mapping

Can **MIT** observations be used to monitor plumes?

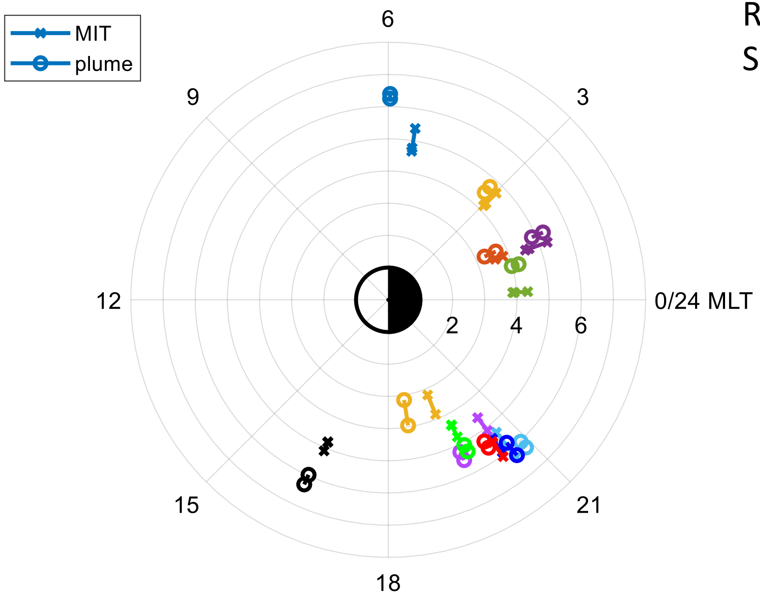

RBSP plume boundaries
Swarm MIT minima and poleward wall (mapping: IGRF)

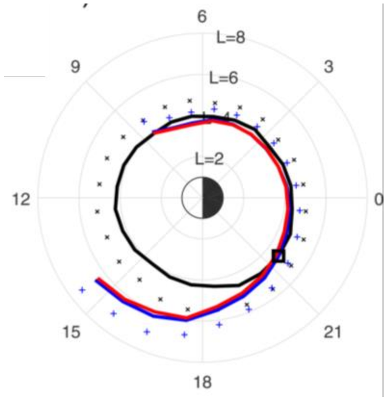

Magnetosphere-Ionosphere coupling

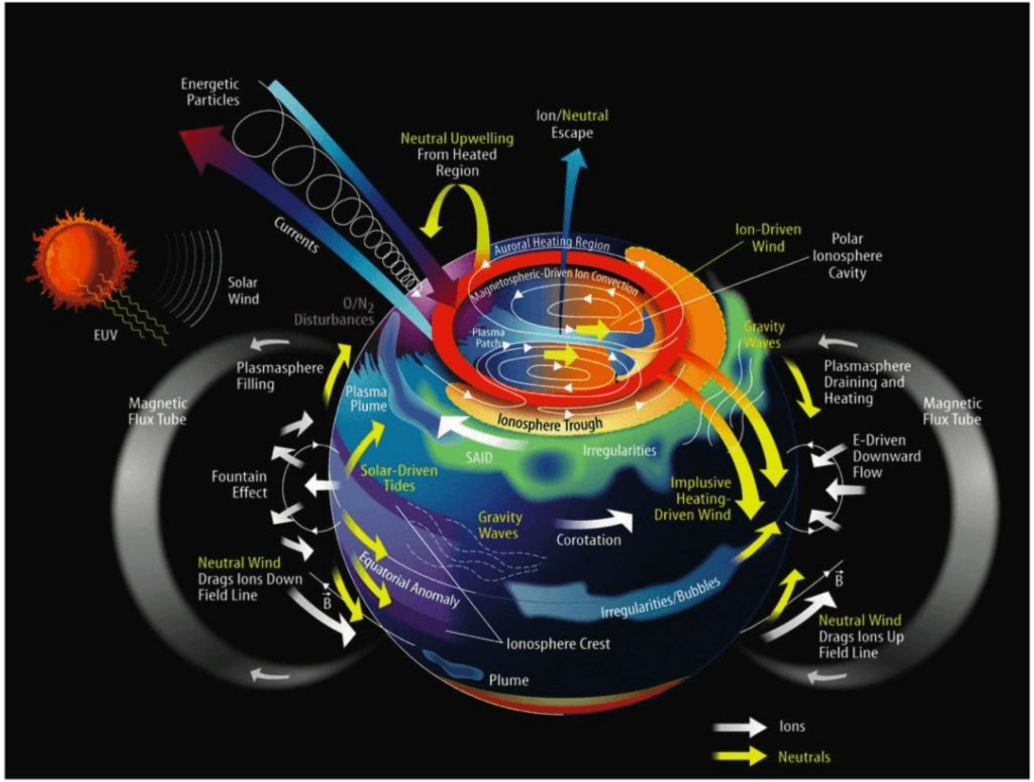

MI coupling is manyfold involving

- magnetic field
- electric field
- electric currents
- particles at various energy
- waves
- heat
- etc.

and these are also coupled to each other